Review Article

Michal M. Godlewski*, Jaroslaw Kaszewski, Paula Kielbik, Jaroslaw Olszewski, Waldemar Lipinski, Anna Slonska-Zielonka, Julita Rosowska, Bartlomiej S. Witkowski, Mikolaj A. Gralak, Zdzislaw Gajewski, and Marek Godlewski

New generation of oxide-based nanoparticles for the applications in early cancer detection and diagnostics

Abstract: Hereby the possible applications of oxide nanoparticles in the cancer diagnostics and therapy are presented. Cancer diseases are nowadays one of the most common causes of death in the highly-developed countries. Discussed will be the current clinical cancer detection methods with their shortcomings. The role of nanomedicine in cancer medicine and the potential applications of nanoparticles debated in the literature will be critically evaluated. In the second part, the most common methods for the nanoparticle synthesis will be discussed. Finally, the system for cancer detection based on the enhanced permeation-retention of multimodal high-k oxide nanoparticles doped with lanthanides will be proposed for both for the magnetic resonance imaging (non-gadolinium contrast agents) and for fluorescence guided biopsy and surgery.

Keywords: medical nanoparticles; cancer diagnostics and therapy; enhanced permeation and retention (EPR); multimodal oxide nanoparticles; lanthanides; fluorescent contrast; MRI

1 The importance of early detection

The increased risk of cancer development is associated with civilization advance and the longevity of the population within the most developed countries of the world. According to the recent reports of various government and private organisations from around the world, this phenomenon was linked with life-style, environmental pollution and, inquiringly, with the development of new, better diagnostic methods [1–3]. Most alarmingly, the life-time risk of developing cancer nearly doubled within the last 40 years, and is nowadays estimated around 40% marker for the general population in the developed countries. However, the majority of tumours are still diagnosed at surprisingly late stages, resulting in the low 5-years survival rate. Present data indicate that 5-years survival rate increases to nearly 100% *i.e.* in the case of an early detection of melanoma. It drops to 62% when the disease reaches lymph node and down to 15%, when illness spreads to different organs. This explains the need for screening meth-

Paula Kielbik, Anna Slonska-Zielonka: Department of Physiological Sciences, Faculty of Veterinary Medicine, Warsaw University of Life Sciences-SGGW, Nowoursynowska 159, 02-776 Warsaw, Poland; Veterinary Research Centre/Centre for Biomedical Research, Department of Large Animal Diseases with Clinic, Faculty of Veterinary Medicine, Warsaw University of Life Sciences-SGGW, Nowoursynowska 100, 02-797 Warsaw, Poland
Jaroslaw Olszewski, Waldemar Lipinski, Zdzislaw Gajewski: Veterinary Research Centre/Centre for Biomedical Research, Department of Large Animal Diseases with Clinic, Faculty of Veterinary Medicine, Warsaw University of Life Sciences-SGGW, Nowoursynowska 100, 02-797 Warsaw, Poland
Julita Rosowska, Bartlomiej S. Witkowski, Marek Godlewski: Institute of Physics, Polish Academy of Sciences, Al. Lotnikow 32/46, 02-668 Warsaw, Poland
Mikolaj A. Gralak: Department of Physiological Sciences, Faculty of Veterinary Medicine, Warsaw University of Life Sciences-SGGW, Nowoursynowska 159, 02-776 Warsaw, Poland

*Corresponding Author: Michal M. Godlewski: Department of Physiological Sciences, Faculty of Veterinary Medicine, Warsaw University of Life Sciences-SGGW, Nowoursynowska 159, 02-776 Warsaw, Poland; Veterinary Research Centre/Centre for Biomedical Research, Department of Large Animal Diseases with Clinic, Faculty of Veterinary Medicine, Warsaw University of Life Sciences-SGGW, Nowoursynowska 100, 02-797 Warsaw, Poland; Email: michal_godlewski@sggw.pl
Jaroslaw Kaszewski: Department of Physiological Sciences, Faculty of Veterinary Medicine, Warsaw University of Life Sciences-SGGW, Nowoursynowska 159, 02-776 Warsaw, Poland; Veterinary Research Centre/Centre for Biomedical Research, Department of Large Animal Diseases with Clinic, Faculty of Veterinary Medicine, Warsaw University of Life Sciences-SGGW, Nowoursynowska 100, 02-797 Warsaw, Poland; Institute of Physics, Polish Academy of Sciences, Al. Lotnikow 32/46, 02-668 Warsaw, Poland

ods and importance of early cancer detection. The most commonly used cancer detection methods include: a) CT scans (X-rays tomography), b) biopsy, c) optical tomography, d) magnetic resonance imaging (MRI) and e) nuclear medicine scans (PET). Yet, practically none of those methods is a really early detection method. Below, some limitations of each above-mentioned methods are listed. These are except nuclear medicine methods, which are less spread, before concentrating on the optical methods based on use of fluorescence markers (labels), the scope of this research.

1.1 In-situ detection – X-ray tomography

Tumour (usually already in the lymph node stage) can be detected by X-rays and localized using tomography. In the latter case large number of X-ray scans is performed. One must, however, take into account the exposure risk linked to X-ray diagnostics. In the consequence, it was estimated that about 0.4% of cancer cases in the USA was a consequence of X-rays scans performed in past! With the (ab)use of X-ray tomography, it is predicted that this will soon rise to 1.5 – 2%. Hence, this method of cancer detection should be used carefully.

1.2 The biopsy – a method of reference

This is the only method that allows identification of cancer type and stage of development following earlier detection of malformations. After resection of tiny portion of abnormal tissue via needle aspiration, a soft tissues pathology is utilised to verify tumour presence. However, the most severe limitation for this method are scarcity of obtained material and possible leakage of cancer cells during palpation and acquisition procedures. Firstly, the needle needs to be inserted throughout the most representative parts of tumour. Since cancers are a strongly polymorphous tissues with common areas of necrosis loci, it is relatively difficult to fully characterise them based on one biopsy, so commonly, material is taken in duplicate or triplicate. Secondly, the risk of cell leakage increases significantly with each procedure and cancer progression. Therefore, a search for new methods for precise delineation of tumour area continues.

1.3 Optical biopsy – a novel detection method

This is relatively new detection method developed specially for mammography. It is based on the fact of detection of a contrast between different elements/tissues present in our body. It is known that fast progressing tumours have a large concentration of blood vessels, allowing a contrasts in the process of red light penetration through a body. Even though the method works, it does not confirm cancer presence, only defines its possibility, furthermore it usually detects already localized and well developed cancers, thus it hardly can be included in the list of early detection methods. However, the use of optical biopsy in mammography is highly advantageous, as compared to its most commonly used alternative, an X-rays mammography.

1.4 Detection of free tumour cells

Tests based on the detection of circulating tumour cells (CTCs) in the peripheral blood or other bodily fluids are at present not conclusive. They only give 80% detection level in the case of metastatic cancers, but in the case of localized, pre-metastatic tumours the threshold drops to only 47%. Similarly with urine, the detection of prostate cancer in the early-development stages is practically impossible, and only in the later pre- and metastatic stages the method could be considered relevant. As such those methods could not be considered for early stage detection. To enhance specificity and increase detection chance of early tumours, a modifications of the test were proposed. The more sensitive early detection can be achieved by introduction of fluorescence labels (FLs). This can be done by labelling CTCs, with antibodies conjugated to fluorochromes or quantum dots (QDs). Secondly, the chance of capture of CTCs can be greatly increased by their binding to magnetic nanoparticles (MNPs), *e.g.* colloidal Fe-based NPs conjugated with antibodies anti-EpCAM. However, the biggest advantage and disadvantage of these methods is the specificity of the utilised antibody. In other words, when antibody against the antigen specific for the tumour is used the results are great, however, as the tumour antigenicity varies (even within the single tumour), the method could give false-negative diagnosis [4–6].

Regardless of the fact, fluorescence markers (labels) for optical detection of tumour or CTCs seem to be especially attractive and thus this review is concentrated on use of fluorescence labels.

1.5 Enhanced permeability and retention effect

The use of small particles (QDs or nanoparticles (NPs)) for tumour targeting could be possible due to the physical properties of the cancer tissues. Enhanced permeability and retention effect (EPR) leads to the accumulation of nanomaterials of certain size in the tumour locus, deposited due to the alteration of the blood-tissue barrier [7, 8]. In the fast-growth of tumour tissue imposes ischaemic conditions within tumour bulk leading to the enhanced vascularisation signalling and accelerated ingrowth of new blood vessels. Such vessels are characterised by more permeable endothelial barriers than in the healthy tissues, allowing the leakage of nanoparticles out of the blood vessels. Secondly, tumour sites are characterised by under-developed lymphatic drainage system, which leads to subsequent nanoparticle-accumulation for prolonged periods. This permeation and accumulation of fluorescent particles could enable fluorescence guided biopsy or fluorescence guided surgery (FGS), a medical imaging techniques with real time visualization of the tumour spread in the diagnostic / operating fields [9]. The FGS potential lays in a fast delineation of the borders between tumour and the healthy tissue, allowing to remove all cancerous tissue while preserving the most of healthy areas, a property extremely important in regards to non-regenerating tissues like brain, lungs, etc. [9]. While other imaging techniques such as magnetic resonance imaging (MRI), computed tomography (CT), and positron emission tomography (PET) also can highlight the location of cancerous tissue but only before surgery. In the consequence, during the procedure, surgeon relies only on pre-made models of tumour, which usually is highly insufficient. Thus, either a significant volume of healthy tissue is removed (high tumour margin), or when this is impossible, usually some cancer is left in situ. As a consequence, it was estimated that about 14%–50% of patients require subsequent re-excision (for reference see [9]).

1.5.1 Fluorescence labels

1.5.2 Problems with organic bio-markers

There is extremely long list of available organic fluorescence labels (FLs), which can be potentially used for biomedical investigations [10]. Their emission in a wide spectral range is possible and is extensively used in the biomedical research. However, organic FLs used in the research have several limitations when applied for in-vivo imaging. First problem relates to the fact that most of organic dyes are characterised by relatively wide light excitation and emission spectra frequently overlapping with tissue and, especially, erythrocyte auto-fluorescence excitation bands. Since living tissues can give high fluorescence signal (especially in the commonly used green and red emission spectra), marker-specific FL emission is often below the level of detection. The only available solution to this problem is evaluation of fluorescence life-time (by fluorescence life-time microscopy, FLIM), where tissue auto-fluorescence is characterised by extremely fast fluorescence life-time when compared to the typical FLs. Unfortunately, FLIM is a relatively costly and time-consuming method, thus it is impractical for real-time applications like FGS. The second limitation of FLs relates to the phenomenon of photo-bleaching caused by irreversible modifications in covalent bonds induced by transition from a singlet state to the triplet state of the dye. Since the process directly relates to dye excitation it cannot be avoided. Thus upon light excitation FL emission is gradually decreased until totally quenched. This, in a specific, narrow research field could be utilised for fluorescence recovery after photo-bleaching (FRAP) experiments for the determination of the diffusion kinetics through the tissue or cell. However, for most cancer-related applications, photobleaching poses a serious problem like, for example, the information on CTCs could be lost if marker stops to emit. Thus many of organic dyes could be used only within so-called photo-stability time (time after which emission intensity is reduced by half), a parameter highly-dependent on the intensity and duration of dye excitation. Another problem with organic FLs lays with the phenomenon of energy transfer (FRET), when fluorescence emission spectrum from a dye overlaps the excitation bands of tissue auto-fluorescence. As a result fluorescence signal from the dye is quenched rendering the use of FLs difficult. Finally, the most serious limitation for all fluorescence based diagnostic methods is the relative low penetration of tissues for the excitation light commonly used. Overall, the limitations described above render FLs of highly limited applicability for medical use.

1.5.3 Quantum dots

The use of quantum dots (QDs) as labels for tumours was first demonstrated at the end of XX and beginning of XXI century. Since their properties overcame majority of limitations of organic FLs, QDs were supposed to trigger a medical revolution. The main postulated advantage of QDs was that they were very small (usually made of heavy-metal

based semiconductor compounds), which was considered important for medical applications. Their size was of only a few nanometers *e.g.* 10^3 times smaller than size of white blood cells and is comparable with size of DNA (about 2.5 nm), protein (about 5 nm) and antibody (about 10 nm). Following quantum mechanics rules, a few nanometers size of QDs means that their optical and electronic properties differ from those of larger particles. These properties directly depend on particle sizes. Quantum engineering is then possible - emission frequencies can be precisely tuned by changing the dots' size, shape and material used or its composition. In the consequence, many applications of QDs is possible and this is very active area of the research. Potential applications of QDs include futuristic transistors with gate length of a few nanometers, dye-based solar cells (so-called Graetzel cells), future generations of light emitting diodes and diode lasers, and importantly markers for medical imaging. The latter was a booming area of the research and resulted in hundreds of reports and reviews [11–16].

Regardless of their size, CdTe, CdS and CdSe core usually encapsulated in the ZnO or ZnS shell gave them high fluorescent yield and great photo-stability and no photo-bleaching was observed. It has been even estimated that quantum dots are 20 times brighter and 100 times more stable than traditional fluorescent dyes [17].

In the follow-up, a range of possible medical applications was proposed and demonstrated [18–26]. However, first restriction for medical feasibility came from the excitation spectrum for QDs, within high-energy UV spectrum efficiently absorbed in tissues, thus of low permeability and proven harmful effect. Second limitation came from the method of application. As the formulation of QDs were prepared strictly for intra venous (IV) applications, their surface had to be modified, usually by bio-optimisation with a variety of surface molecules, mainly polyethylene glycol (PEG) or its derivatives [27]. This enabled their stability in suspension and, surprisingly, good penetration to the tumour site. Additionally, the distinctive surface properties of QDs enabled their potential usage in targeted drug delivery, as drug carriers or selective markers, for so called targeted therapy (see *e.g.* [16, 28]. Examples of such use of QDs QD-based multifunctional probes can be found in many of publications (see *e.g.* [29–35]).

First such experiments were performed in 1990 when QDs were introduced for imaging of cancer cells in-vitro [36, 37]. To achieve better selectivity QDs conjugated with cancer specific ligands, antibodies, or peptides were applied, but for *in-vitro* detection of cancer cells [38–45]. This was soon followed by *in-vivo* tumour imaging [46–50].

There are several reasons why semiconductor based QDs (mostly based on CdS and CdSe) are no longer considered as a appropriate choice for a new generation of FLs.

The first is a spectral diffusion relating to a spread of QDs sizes causing spread of both excitation and emission bands. Different line shapes are observed for different sizes of nanocrystals. In the consequence, several groups reported excitation intensity and integration time dependent linewidths [26], a relatively minor physical problem, however of strong importance for diagnostics, as it may affect detection of marker-specific emission. The second problem, fluorescence blinking [51–56], raised from large surface to volume ratio of QDs. A single dot can blink off (emission is quenched) unexpectedly and uncontrollably. Time scale of such emission quenching can vary between microseconds and several minutes, which makes quantitative analyses very difficult. The causes of the blinking are still unresolved and remain the subject of intense studies. This drawback has been solved by some research groups by the introduction of nonblinking QDs [57, 58] with highly complicated core-shell layered systems [59]. Then, enthusiastic reports for future medical use of QDs were quenched when, upon closer evaluation, the tumour targeting phenomena were attributed to the pickup of PEG-orchestrated QDs by white blood cells.

Furthermore, the potential use of QDs in medicine was finally snuffed by the reports of the toxicity associated with the ion leakage from their heavy metal core. The most critical limitation relates to toxic properties of Cd-, Hg-, Pb-based QDs. Unfortunately, such QDs (mostly based on CdSe) show the brightest emission. Such probes exhibited both *in-vitro* and *in-vivo* cell toxicity [60, 61]. Furthermore, their accumulation in the liver and central nervous system combined with nephro- and neuro-toxicity were reported. Numerous works reported toxicity of cadmium. There is no known natural elimination mechanism of cadmium and this metal, as other heavy metals, can accumulate in the organism. Initially, it was claimed that cadmium core was encapsulated within biologically-inert shell thus the toxicity problem was avoided. Unfortunately, it was found that the high energy of UV irradiation was close to that of the covalent chemical bond energy of CdSe nanocrystals. As a result, semiconductor particles were dissolved, in a process known as photolysis, and a release of toxic cadmium ions into the culture medium was confirmed. *In-vitro* studies, based on cell cultures, confirmed toxicity of Cd-based QDs. Mechanism of toxicity is very complicated and depends not only on the content of heavy metal (cadmium) but also on size (later on this problem will be discussed), shape, surface functional groups, and surface charges [62, 63]. Moreover, it was reported that Cd-based

QDs after exposure to light may generate highly aggressive (toxic) reactive oxygen species (ROS) [64]. Finally, the size of the first generations of QDs spelled their doom. Reports showed that the smallest nanocrystals diffused uncontrollably through the cell [65] and accumulated in the vicinity of mitochondria [65] and in the cell nucleus whereupon ROS creation they could induce DNA mutations [66]. In summary, one can conclude that present knowledge about toxicity eliminates use of QDs as markers for biomedical applications. This problem is discussed in details in dedicated reviews on toxicity of QDs with heavy metals [67–69]. To overcome the toxicity problem, a novel approach utilizing second generation of non-heavy metal, low-toxicity QDs [49, 70, 71]. For example, Zn-based QDs were tested for medical applications. Since devoid of toxic core, such QDs became a promising tool for medical applications.

2 Alternative labels

In this chapter, we'll summarize requirements for alternative nanocrystal-based labels for medical applications. Regarding safety aspects, proposed nanoparticles (NPs) should be made of non-toxic components and be of a "proper size" (this fact was often ignored in previous investigations, and will be discussed below). Secondly, regarding detection problems, no bleaching or blinking should occur. Thirdly, to avoid spectral diffusion, the fluorescence emission of dopants should be independent of NPs size or utilized matrix. Emission must be spectrally distinctive, which should help to differentiate between NPs from auto-fluorescence of the tissues. The importance of NPs shape will also be shortly discussed.

2.1 Safety aspects of NPs introduction and elimination

As mentioned above, the majority of studies concerning the *in-vivo* applications of nanostructures were based on their IV administration [72–74]. It can also generate other problems including aggregation of nanostructures or their sticking to erythrocytes causing disruptions of a blood flow, especially in capillaries. Consequently, a strict requirements are imposed on suspension containing nanostructures for IV, with their long-term stability and dispersion at a top-most priority [76]. One of the postulated methods used to overcome described in-suspension stability problems was coating of nanoparticle surface with ionic compounds, like PEG. Unfortunately, this approach lead to

the activation of immune system and subsequent uptake the administered nanomaterials by mononuclear phagocyte system [75]. The limitations of IV route-of-entry hampered a development of NPs for medical applications and prompted a wide search of alternative delivery methods. Hereby, a relatively safe and tested by Godlewski *et al.* [78, 79] is proposed, at least for hydrothermally-produced oxide NPs, method of alimentary (oral) application of nanocrystals. Despite the presence of intestinal barrier in the adult mammals, absorption of molecules from gastrointestinal tract to the blood circulation was confirmed and described as persorption [77]. The applicability of this route for NPs is confirmed, with their rapid intestinal uptake and wide organ distribution and following elimination, including transfer through the tight organ barriers, like blood-brain barrier (BBB) (Figure 1) [78, 81, 82]. Furthermore, active cellular uptake and targeted intracellular trafficking and transport through cells was confirmed. Our initial data suggests that clatrin-mediated endocytosis of nanoparticles proved to be crucial for the transport of nanostructures through the intestinal barrier. However, caveolin-mediated transfer cannot be fully excluded from the process. *In-vitro* studies on the transport of ZrO_2:Tb NPs in the live primary murine neuron culture confirmed trafficking of the NPs via vesicular intracellular trafficking, and their passage in-between neurons [80]. This observations correlated with subsequent study, where alimentary administrated ZnO:Eu NPs were detected and visualized in brain tissue, especially in the areas of limbic neuronal networks system and cerebellum [82]. Crucial questions arose following recent data of the transfer of NPs through BBB following multiple application. Permeability of the BBB seemed finite, thus strict regulation of the uptake of NPs was postulated. Similarly, as essential as NPs uptake, were the concerns of the NPs long-term deposition and their elimination from the organism. It is proved, that following oral administration, from 24 h on, clusters of NPs were detected in the vicinity of hepatic arteries/bile ducts indicating the role of liver, more specifically the bile for oxide NPs elimination from the organism [82]. Furthermore, in the case of ZnO-based NPs the biodegradation of nanocrystal matrix may play a crucial role in their elimination [81].

2.2 Question of size and shape

Differences in the reported distribution patterns of various tested NPs in previous studies can be strongly linked to inconsistencies in the size of utilised nanostructures. Studies with orally administrated gold NPs (size range of 4 to

A

	ZnO:Eu	Y$_2$O$_3$:Eu	ZrO$_2$:Pr	ZrO$_2$:Tb

Liver

Lungs

B   **Primary sites of induced tumours**
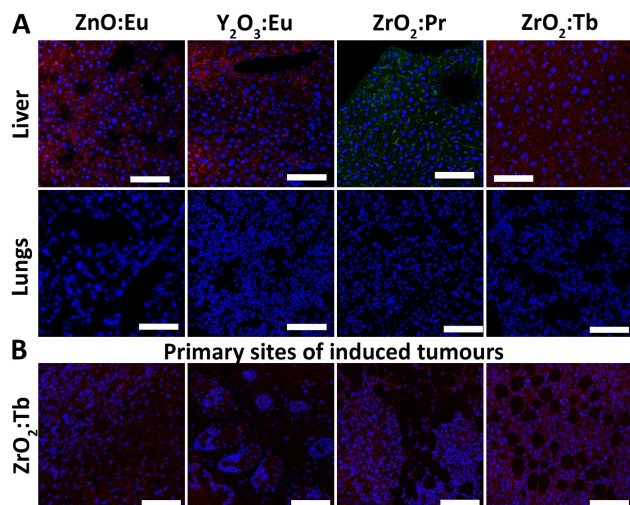
ZrO$_2$:Tb

Figure 1: Organ distribution of oxide nanoparticles doped with various lanthanides (ZnO:Eu, Y$_2$O$_3$:Eu, ZrO$_2$:Pr and ZrO$_2$:Tb) 24h following oral administration of nanoparticle suspension in mice (A). Nanoparticles transferred to majority organs (hereby liver is shown). However, the blood-organ barrier in the healthy lungs proved impermeable, and no nanoparticle-related signal was ever found in this tissue, regardless of time post-administration. For most lanthanides the predominant range of luminescence was within red to far-red spectrum, however for Pr doping, the majority of the signal was found in the green region. Distribution of ZrO$_2$:Tb nanoparticles to primary sites of induced mammary gland tumours (B). Nanoparticle-related signal was observed in various types of tumour tissue from solid, through glandular to the necrotic loci. Bar = 100 nm

48 nm) revealed their distribution to various organs and tissue of mice, among others in the brain. However, their intracellular distribution showed patterns characteristic for simple diffusion, rather than associated with active intracellular trafficking [65]. Active intracellular transport of NPs seems one of the most important issues concerning their applicability for medical applications, as only the intracellularly recognised objects can be trapped and eliminated from the cell and, subsequently, from the organism [65]. On the other hand, smallest nanocrystals, unrecognised by cellular transport mechanisms may allocate in the cells and tissues indefinitely. The persistence of NPs in the tissues could result with a combined negative effect, a possibility of cumulative or chronic toxicity, as well as the question of "background" noise from previous applications that could strongly distort the results of future medical examinations.

Despite the importance of NPs size in the mechanism of their distribution in the living organism, the shape of tested material seems also of importance. Previously studied Y$_2$O$_3$-based NPs with elongated shape (width of around 100 nm and length of up to few μm) indicated trans-

fer to tested tissues following IG, however, the effectiveness of this transport was reduced when compared to the smaller, oblong ZrO$_2$ or ZnO-based matrices. Compared in the study commercial NPs with different shape did not reveal any accumulation in examined tissues [79]. Likewise, ZnO-based NPs showed increased ability to transfer through physiological barriers (*i.e.* BBB) and improved short-term accumulation in tested organs [81].

2.3 A promise of rare-earth oxide NPs

Rare earth (RE) ions, observed mostly in 3+ charge state, showed sharp atomic-like photoluminescence (PL) and PL excitation (PLE) bands. This was attributed to screening of internal 4f shell by electrons from filled $5s^2$ and $5p^6$ shells (Figure 2). Energy levels seen on diagrams result from electronic [Xe]$4f^n$ (n=0-14) configurations of Ln^{3+} ions [84]. An important consequence of the screening was host independent emission, reported crystal field effects were small. Emission wavelength was also strongly independent of host particle size. Thus, spectral diffusion of excitation, a huge problem for early NPs and QDs was avoided. The use of larger (biologically-preferable) particles also solved other limitation of QDs and blinking was not observed. Unfortunately, purely atomic-like characteristics of 4f shells meant that 4f-4f excitation and emission processes were parity forbidden. Hence, particles activated with RE ions were not as good emitters as QDs. Detail discussion of possible excitation and emission processes was given in the reference [83]. On the other hand, parity forbidden character of 4f-4f transitions could also be advantageous. Reported PL decay time was usually in microseconds time scale, *i.e.* it is about 1000 times longer than for cells autofluorescence. This, could potentially allow, separation of label and cell emission by the time-resolved PL, with the limitations described above. However, this also implicates that excitation energy can be reduced to minimize danger of phototoxic effect for cells, in particular when short wavelength excitation is applied.

2.4 Biomedical labels

Fluorescence is emission of light due to allowed electronic transitions, while phosphorescence, by definition, uses forbidden transitions between ground and excited states [85]. The main experimental difference lies in the lifetimes of both phenomena, as the former exhibits short times ca. 10^{-8} s and latter shows long times in the range milliseconds to seconds. For biological application mainly
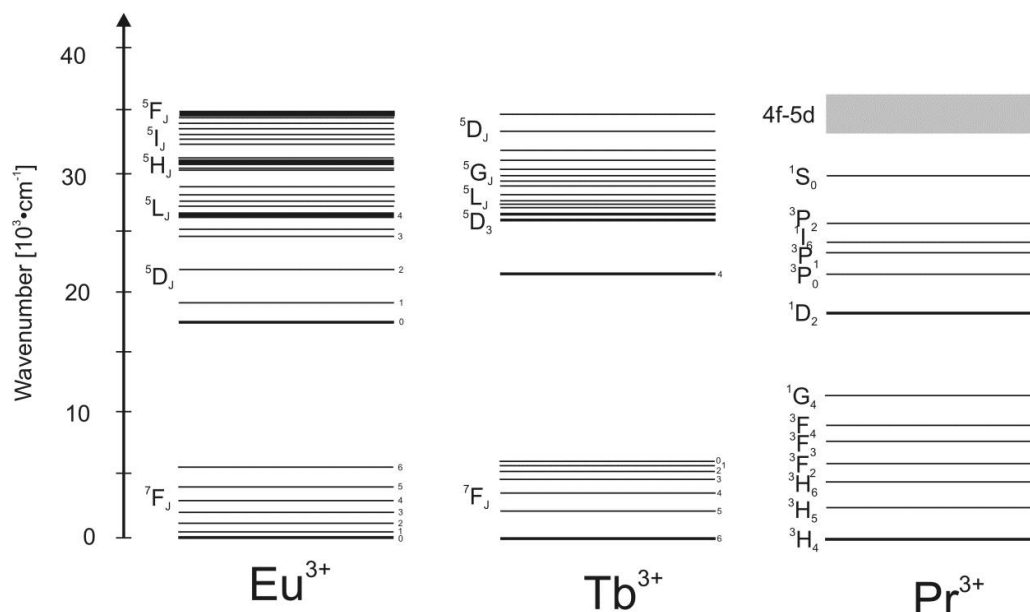
Figure 2: Energy level diagrams of Eu^{3+}, Tb^{3+} and Pr^{3+} ions [84]

fluorescent organic dyes are used, which exhibit relatively high efficiency and high selectivity of labelling [86]. However, some phosphorescent dyes are also used, usually complexes of transition metals [87–89]. The separate category consists of luminescent nanoparticles, which may be split into several branches: inorganic, organic and hybrid nanoparticles. Inorganic nanoparticles may be divided into categories: semiconductor QDs, metallic NPs, nano-carbon, oxide NPs and others. Organic nanoparticles may be split into fluorescent organic nanoparticles (FONs), polymers and protein nanoparticles. Furthermore, hybrid nanoparticles category, consisting of inorganic-organic composites was recently developed [90–92].

2.5 Nanoparticles in medicine

Nanoparticles could potentially find applications in a variety of medical areas, from which one of the most important is drug delivery. As pointed by Kumar *et al.* [93] there are certain properties a candidate for drugs has to fulfil: biocompatibility, ability to release drug, targetability, control over time of delivery and the route of administration. As discussed above, ability to deliver compounds into the living organisms, through the organ barriers, with high preference of tumour sites, renders NPs, especially non-toxic oxide-based, a promising tool for diagnostics and therapy. One of the most discussed form of NPs application in medicine is photodynamic therapy [94]. There are several of advantages when NPs are used in this kind of treat-

ment: they can carry large amount of photosynthesizer, they prevent preterm release of photosynthesizer, they can be surface functionalized, can carry multiple components, finally they localize in the tumour. Furthermore, the fluorescence of the nanoparticle itself can be utilised to trigger the activation of the photosynthesizer through the energy transfer phenomenon. Unfortunately, the strongest limitations for the use of NPs for phototherapy are the delivery route (mentioned above limitations of the IV route-of-entry) and the limited penetration of excitation light through the tissue. As such, existing NPs could only be utilised for the treatment of surface tumours. To overcome this limitation an approach through up-converting NPs will be discussed below.

Second growing demand where NPs could be utilised in the treatment is tracking of the drug delivered into the organism. From plenty of fluorophores classes, the two main groups are considered for this applications: endogenous and exogenous imaging agents [95]. Former are primarily fluorescent or luminescent compounds activated by drug-triggered enzyme activity inside the investigated organ and the latter are luminescent substances introduced with the drug. Best known endogenous agents are green fluorescent proteins (*i.e.* GFP, RFP, etc.) and luciferin. They offer low photobleaching, but have other significant drawbacks as both need to be delivered in the form of genes into the living tissue. Furthermore, the intensity of luciferin luminescence is rather low, requiring long exposure times. Thus luciferin cannot be applied for the study of dynamic processes. Exogenous imaging agents include

all kinds of foreign substances with: colorimetric, luminescent, magnetic or nuclear contrasting properties, administrated to living organism for the sole purpose of observation. Amongst exogenous agents most frequently listed were gold nanoparticles (AuNPs), semiconductor quantum dots (QDs), superparamagnetic iron oxide nanoparticles (SPIONs), carbon nanomaterials and nanoparticulate silica [96–98]. Noble metals nanoparticles exhibited useful luminescent properties related to surface plasmon resonance (SPR) phenomenon. As the mean electron path is longer than particle size, the confinement effect occurs. Rapid luminescence strength increases, when the particle size is below 2 nm. Quantum dots exhibit strong confinement effects found in semiconductor crystals with sizes below certain point, which is related to strong luminescence. Carbon based imaging agents, either carbon dots [100] or some forms of graphene [99] were also postulated. Mechanism of photoluminescence in carbon dots is related to existence of intrinsic bandgap, creation of the trap states related to the doping of the carbon dots or presence of the luminescent molecules in the structure of the carbon dot [100]. Graphene quantum dots are known for intrinsic luminescence and were proposed for biological imaging. Doping in with nitrogen resulted in their high activity in two photon fluorescence imaging [101]. Also, composites of graphene with semiconductor quantum dots were applied in biological imaging [102]. Regardless of the intensive research, neither of the above-mentioned exogenous imaging agents found their way into medical applications. For QDs and AuNPs the reported toxicity spelled doom [103–106]. Similarly, reports of toxicity for nanocarbons rendered them useless [107–109]. For now, the most promising are SPIONs, mostly considering their magnetic properties.

sorbed and not related to the thermal population of higher levels [113]. Up-conversion was since found in semiconductor nanoparticles and lanthanide-doped nanoparticles, however the process was not limited to these classes. Many mechanisms of up-conversion, were postulated from which the most important are: energy transfer up-conversion (ETU), excited state absorption (ESA), cooperative sensitization, cooperative luminescence, second harmonic generation (SHG) and two photon absorption (TPA). Mentioned processes efficiencies differ from 10^{-3} for ETU mechanism to 10^{-13} for TPA. Efficiency depends mainly on the relative location of the energy levels and phonon frequencies of the host lattice. The most suitable host lattices in lanthanides activated up-conversion were fluorides as they exhibit low phonon energies and thus minimize nonradiative loss [114]. However, fluorides are known for their toxicity in the living organisms [115, 116]. Besides fluorides, other up-converting halides were discussed [117, 118]. Efficient up-converting nanoparticles may be also based on oxyfluorides, oxides and perovskites, when doped with appropriate lanthanide ions [119]. Lanthanide ions are the most promising, since several of them are considered of minimal toxicity, even though their luminescence yield is relatively low. The main problem with low efficiency of lanthanide-doped oxides was overcome by preparation of core-shell nanoparticles, coating techniques or post-annealing processes [120]. A number of matrix compounds were tested and found to exhibit strong Er or Er/Yb activated up-conversion, *i.e.* YOF [121], Lu_2O_3 [122], TiO_2 and $BaTiO_3$ [123], Gadolinium-Galium-Garnet (GGG) [124] and more complex oxides like $K_2La_2Ti_3O_{10}$ [125]. Therefore, many lanthanide-doped oxide nanoparticles found their applications in the imaging [126]. For further information concerning up-converting nanoparticles [127–130].

2.5.1 Up-converting nanoparticles

From exogenous inorganic imaging agents, the up-converting nanoparticles are of the special interest [99]. The main limitation of single-photon fluorescence for medical uses is the depth of the penetration of the excitation spectrum in the tissues ranging from around 50 nm (for UV) to 200-300 nm for blue, green and red spectra. Since up-converting agents rely on the infra-red excitation the efficient penetration window increases even up to cm, the range suitable for some medical applications. Phenomenon of up-conversion was first observed in nineteen sixties, there have to be mentioned authors: Franken [110], Bloembergen [111] and Auzel [112]. The process is related to emission of photon with higher energy than photons ab-

2.5.2 Nanoparticles doped with lanthanides

Nanoparticles doped with lanthanides are gaining popularity. Nowadays lanthanide-doped fluorides, oxides [131], polymers [132], functionalized nanoparticles [133] and up-converting nanoparticles [134] are discussed. Lanthanide ion-doped nanoparticles are considered for their luminescence, as well as for their activity in nuclear magnetic resonance imaging. In luminescence imaging they can also be used as infrared emitting phosphors and as multimode contrasts agents [135]. A lanthanides emission spectrum is well defined and does only weakly depend on the crystalline environment of the ions. Lanthanides offer a sharp lined emission spectra, a consequence of electronic transitions within f-manifold [136]. Furthermore, of high medical

interest, is the fact that spectrum of lanthanide ions contains many excitation-emission lines, some of which are available in the visible region [137].

2.6 Synthesis of luminescent nanoparticles, top-down and bottom-up methods

The two main philosophies of nanomaterials synthesis are top-down and bottom-up. Top-down approach offered synthesis of nanoparticles by fragmentation of bulk material with classical methods to achieve the nanometre sizes. Utilized methods included high energy ball milling, plasma etching, lithography techniques and anodization [138]. On the other hand, the bottom-up technique is based on the assembly of fundamental chemical entities like atoms, ions or molecules into the nano-size objects. As this technique provided pure materials of defined shapes and sizes and the processes could be easily controlled, tuned and modified, the bottom-up approach will be discussed in this paper. Generally, the bottom-up synthesis could be divided to three general categories: physical methods, biological methods and chemical methods, discussed below.

2.6.1 Physical methods

The most commonly used physical methods of nanoparticle synthesis were: physical vapor condensation and spray based methods, as well as ultrasound assisted processes. Despite the fact that described methods were of physical character, some of them induced or sustained chemical reactions.

Vapor condensation techniques
Generally, gas condensation methods were the most common physical methods of NPs synthesis. Here, the precursor was evaporated in either inert or reactive gas and then condensed to form nano-structures [139–141]. The inert gas was most commonly used for the synthesis of metal and metal alloys nanoparticles [142], the reactive gas allowed crystallization of compounds [143]. When precursor was difficult to evaporate, pulsed laser ablation was utilised to perform transition to the gas phase [144]. To form more complex compounds, chemical vapor deposition method (CVD) was used, where reaction of various precursors occurred in the gaseous phase [145], usually in reduced pressure atmosphere (pyrolysis) [146]. In the spark discharge synthesis, the precursor released from the electrode formed metal nanoparticles which then re-

acted with gas to form compound nanoparticles [147]. Photothermal pyrolysis was a variant of vapor condensation method, where precursors were rapidly heated using infrared laser, allowing faster synthesis and smaller nanoparticle sizes [148]. The thermal plasma synthesis method was preferable for materials with high melting point. The high temperature of plasma arc, ensured the evaporation of precursor to the supersaturated state from which nanoparticles were formed through the nucleation and condensation processes [149]. In flame synthesis method, vaporized metallic compounds, usually halides or alkoxides, were oxidized in the flame to form the oxide nanoparticles [150]. Finally, one of the more interesting vapor condensation method of semiconductor nanoparticle synthesis was a low temperature reactive process. There, precursors were vaporized and reacted without additional heating of a flow gas, the heat produced by the reaction itself being sufficient for crystallization [151].

Spray techniques
The spray techniques were also commonly employed for the production of nanoparticles. One of the most popular method was spray pyrolysis method [152], where metals solution is atomized. Then resulting droplets are introduced into the furnace, where solvent was evaporated and precipitate of precursor reacted with surrounding gas, decomposed to form product, which may undergo further sintering. A variant of this method employed the plasma arc instead of the furnace [153]. Conductive solution could also be atomized using electric field of several kV in the electrospray pyrolysis method. The advantage of this method was a strict control of the droplet size in the range from few nanometres for liquid metals to hundreds of micrometres for dielectric liquids [154]. Following atomization of solution, a typical 'droplet to particle' conversion process occured. In low pressure spray pyrolysis (LPSP) technique, droplets of the solution were introduced into low pressure chamber, which promoted fast solvent evaporation and rapid nucleation to primary nanoparticles. Afterwards, gas was rapidly released from the primary nanocrystals, facilitating their fragmentation into the final product. In a conventional spray pyrolysis process, product underwent aggregation resulting in the formation of three-dimensional networks. To avoid this, salt was introduced into the solution to coat the surface of single nanoparticles and inhibit agglomeration. In, thus called, salt-assisted spray pyrolysis method, salts were easily removed from the nanoparticles by washing, leaving non-aggregated nanoparticles as a product. As a result, size distribution was significantly improved, with

nanoparticles exhibiting mono-dispersity [154]. Other variant of this method was spray drying technique [155], where starting solution was already a colloid of primary nanoparticles, which was rapidly dried after nebulization into the chamber with hot inert gas. Nanoparticles could also be long-term stabilized by freeze drying method [156], where the suspension of nanoparticles was frozen, then the solvent was sublimated under reduced pressure.

Ultrasound assisted methods

Methods of nanoparticles synthesis based on the ultrasound treatment relied on the phenomenon of acoustic cavitation [157]. This process involved formation, growth and implosion of bubbles, related to creation of local extreme conditions. Hot spots inside the bubbles had temperatures of thousands degrees K with extremely steep heating and cooling rates, furthermore implosion was associated with generation of a pressure wave, as high as 1000 bar. Finally, implosion of the bubbles caused thermal dissociation (sonolysis) of the water molecules with generation of free radical species [158]. These extreme conditions were perfect for synthesis of new materials and ultrasound had both physical and chemical impact on preparation of nanostructured materials. Ultrasound has been reported to influence variety of factors in sonochemistry [159]. The use of ultrasound effects on the reaction mixture included increased reaction kinetics, changes in the reaction mechanism, enhanced precipitation and crystallization [160]. The use of ultrasound in electrochemistry resulted in separate branch of synthesis – sono-electrochemistry [161], with pure metals, alloys, semiconductor crystals and oxides proved viable for sono-electrodeposition. Other variant of the method was sono-chemical reduction of metal salts in solution [162] with pH considered the fundamental controlling parameter of the process [163]. Generally, sono-chemical deposition allowed to achieve uniform nanoparticle coatings [164].

2.6.2 Biological or bio-assisted methods

Synthesis of the nanoparticles may also be performed with the use of living organisms. There were successful attempts to crystallize metallic nanoparticles using bacteria, fungi and plants [165]. Nanoparticles of Au, Ag, Pt, Pd were prepared intra- or extracellularly, mainly by biosorption-reduction mechanism. Intracellular mechanism was associated with attraction of positively charged metal ions into the negatively charged cell walls. Then, enzymes capable of conversion of the ionic form of metal into nanoparticles

diffused through the cell wall [166]. Extracellular mechanism was related to the reduction of the metal cationic form, with many prokaryotic or fungi organisms able to exude appropriate enzymes. On the other hand, via the *ex-vivo* approach noble-metal nanoparticles were synthesized utilising plant extracts, *i.e. Ginkgo Biloba* [167] or *Piper nigrum* [168], which acted as reductants and stabilizing agents. In preparation of gold nanoparticles, extracts made out of various parts of the plant resulted in creation of products of many shapes and sizes [169]. Another approach assumed mimicking of the biomineralization processes, where the organic substrate was synthesized, or chemical precipitation method was used on the bio-templates [170, 171]. Microorganism-mediated synthesis of nanoparticle metals, alloys, oxides, sulphides and carbonates was found to be controllable by pH, temperature and concentration of precursor compound [172]. Nanoparticulate silica was synthesized using BKH1 bacteria using magnesium trisilicate or tetraethyl orthosilicate precursors [173]. Also many metallic, oxide and sulphide NPs were synthesized using variety of bacteria strains [174, 175]. Similarly, fungi were applied in nanoparticles synthesis as they were able to produce great quantities of enzymes, which were, beneficially, more resistant to the mechanical conditions in bioreactors making them appropriate for large-scale production [176]. Finally, a great advantage of nanoparticle biosynthesis is utilisation of the waste materials as precursors [177].

2.6.3 Chemical methods

Chemical methods of bottom-up synthesis of nanoparticles are by far the most popular. Generally they could be divided into three main reaction groups: gaseous phase, solid phase and liquid phase reactions. Gaseous phase reactions were already described along with vapor condensation techniques (2.6.1.1. unit).

Solid phases reactions

Solid state synthesis employed direct reaction of solid precursors, usually at high temperature [178]. Method may be used to design new compounds [179], as well as the synthesis, of crystallized nanoparticles of metals, alloys [180], inorganic ionic compounds [181–183], and complex oxides [184]. Synthesis may be performed starting from both inorganic [185] or organic [186] precursors.

Combustion synthesis, a self-sustaining process, relied on exothermic, usually very fast, reactions [187]. It was subdivided into two categories depending on the way the

process was ignited. The first was called thermal explosion. The reactants were heated and reacted spontaneously in all the volume to form product. The second was called self-propagating high temperature synthesis (SHS) and it initiated locally, self-propagating from the source through the whole available precursors. SHS process was mass and energy transport limited, also many variants of the method were described [188]. Method was suitable for synthesis of ceramic powders and composite materials [189]. It exhibited numerous advantages, with high purity of products, high reaction rates, possibility of metastable phase synthesis and densification of product mentioned as the key ones, along with possibility of synthesis of novel nanomaterials [190]. Through these processes, mechanically structured materials, nanopowders, energetic materials, microelectronics soldering components, multilayer reactive nanofoils were successfully created [191].

Second group, the mechanochemical reactions, were activated by high energy ball milling (HEBM) [192]. There, mass and energy transfer was reported happening without the use of liquid solvents. Many classes of materials that can be synthesized by this method: metal nanoparticles [193] metal organic frameworks (MOFs) [194], composite nanomaterials, metal oxide nanoparticles [195] and others [196]. As an example, zinc sulphide quantum dots were synthesized this way from zinc acetate and thioacetamide [197] and silver chloride nanoparticles were produced using NH_4Cl, $AgNO_3$ and NH_4NO_3 as substrates [198].

Liquid phases reactions

By far the most common chemical method of NPs synthesis utilised liquid reaction phase. Sol-gel technology was known from 19th century [199] and have been used for preparation of materials, including thin films, fibres, glasses and ceramics from solution. The main advantage of the method was that precursors were mixed at molecular level in low temperature, to form a product. Typical sol-gel process included four steps of preparation [200]: solvolysis, condensation, solvent removal and thermal processing. At the stage of solvolysis metallic compounds were transformed into hydroxide, and sol was created. Then metal-oxygen network was created and sol condensed to form gel, which was dried slowly to remove the solvent. At the last step, which took place at the elevated temperature, the network was decomposed to form a final product. Sol-gel technology may also be combined with other techniques like solvothermal method, spray drying, phase separation, atmospheric pressure drying, surface modification and emulsion process to produce new unique nano-

materials [201]. With support of sol-gel technique there was possibility to synthesize inorganic-organic composites [202, 203]. Technique was used to synthesize nanomaterials using templates [204] and cooperative assemblies of templates and building blocks [205]. The method was suitable for synthesis of metal oxides [206], metal nitrides and carbides [207], semiconductor quantum dots [208] and metal organic frameworks [209]. Pechini synthesis was built on principles of sol-gel chemistry and assumed synthesis of metal-citrate complexes, which were then polymerized [210, 211]. Method was successfully applied in the synthesis of luminescent materials [212, 213]. Final advantage of these methods allowed direct observation of the crystallization in the sol-gel with *in-sit*u methods [214].

Second chemical method of NPs creation is solvothermal method. Solvothermal process is general term describing a technique of materials synthesis at conditions of elevated temperature and pressure [215]. By definition, it is chemical reaction taking place above the room temperature and at pressure greater than 1 atm, occurring in closed container [216]. Act of crystallization may take a place in water, then it is called hydrothermal or in other solvent [217, 218]. Reactions are performed in closed autoclaves, where reaction mixture is heated [219]. Hydrothermal method offers possibility to synthesize new phases or new complexes, nanoparticles and crystals of many inorganic compounds [220]. It also enables control over shape and size of the product grains [221]. New materials may be produced that way, including nanoparticulate transition metals oxides [222, 223] microporous crystals, superionic conductors, complex oxide ceramics, fluorides, magnetic materials, luminescence materials, inorganic-organic hybrid materials [224]. At hydrothermal conditions metal salt undergoes hydrolysis with formation of metal hydroxide, then condenses to form metal oxide or metal nanoparticles [225]. Hydrothermal nanoparticles synthesis experiment can be planned basing on the thermodynamic considerations [227]. Hydrothermal process may be periodic as well as continuous [228], and the latter is easily transformed into industrial scale production and offers significant reduction in energy usage and thus overall costs.

There is variant of the method, where the reaction mixture is driven to supercritical conditions. During phase shift of the regular solvent to the supercritical fluid, its properties rapidly change, *e.g.* dielectric constant being one of the most important solution parameters in nanoparticulate materials synthesis [229]. In naturally occurring hydrothermal vents natural conversion of simplest chemical compounds (*e.g.* CO_2, CH_4, NH_3) transpires, with resulting, more complicated molecules, becoming a food source for various organisms [230]. The opposite is also possi-

ble, hydrothermal processing may cause decomposition of complicated compounds to form simpler ones. This fact is used in processing of biomass to obtain bio-oil, bio-gas or bio-carbon depending on the process conditions [231].

Finally, microwave field assisted methods are presented with microwave hydrothermal method of materials crystallization. The focus, would be a synthesis of inorganic compounds. Microwaves are electromagnetic radiation with the wavelengths between 0.001 to 1 m [232]. However only frequencies of 915 MHz and 2.45 GHz were allowed for industrial and domestic use [233]. Microwaves were used for the purpose of heating of dielectric materials. In materials synthesis, it was applied to conduct solid-state reaction between dielectric precursors [234], calcination processes and several other methods of preparation of nanoparticles [235]. Local character of microwaves interaction with chemical bonds was often utilised in microwave irradiation based methods, to produce, among others, carbon nanotubes [236], oxide nanoparticles [237], semiconductor quantum dots [238] and colloidal nanoparticles [239]. Microwave irradiation was also known to induce crystallization of metal and oxide nanoparticles in the presence of reducing agents from plant extracts [240–242]. Examples of indirect microwaves application in nanoparticle synthesis were microwave plasma related methods [243], which included microwave assisted spray synthesis [244], microwave plasma sintering, [245] and many personalized methods like microwave pulsed plasma polymerization [246] or microwave plasma deposition of nanoparticles on substrate [247].

Microwave solvothermal synthesis
The technique

The use of microwaves significantly increased the rate of chemical reaction in our preferred solvothermal processes [248, 249]. Also, the overall purity of product obtained by microwave solvothermal synthesis was much higher than in the conventional solvothermal process, as the heating elements did not have direct contact with reaction mixture. Local interaction of microwaves with precursors allowed crystallization of new and metastable phases. These properties lead to the synthesis of many new materials including carbon nanotubes [250], zeolites [251], composites [252] and semiconductor nanoparticles [253]. Hereby, the oxides synthesis will be discussed in detail, as its products have potential applicability for biological sciences and medicine [254]. Technology of nanometric zinc oxide was established for both nanorods [255] and nanoparticles [256]. Microwave hydrothermal synthesized oxides had significantly higher structural quality

compared to those from chemical precipitation or calcination [257]. Furthermore, microwave hydrothermal synthesized oxide nanoparticles, were easily doped with lanthanide ions, for the visible region excitation-emission of luminescence [258–260]. Conditions of oxide crystallization in microwave driven hydrothermal process had a strong influence on the product properties [261, 262]. Also, phase composition was influenced by post processing of obtained nanoparticles [263, 264]. The most biocompatible materials produced using microwave solvothermal approach were oxides. Hereby, a successful attempts to crystallize new generation of nanoparticles exhibiting optical [265, 266] and magnetic [267, 268] properties are presented. All of which were a wide bandgap semiconductors or dielectric materials. Additionally, a redox behaviour was investigated in our products [269]. Later, it will be discussed the biocompatibility of microwave hydrothermally grown oxide nanoparticles doped with lanthanide ions as they were extensively tested *in-vivo* in the acute, chronic and multiple exposure modes in mice [270–272]. Application of water as solvent ensured that nanoparticles were terminated by hydroxyl groups, which made them an ideal candidates for surface modifications by bioactive compounds for the applications as a drug carrier [273]. Finally, initial studies in the applicability of the lanthanide-doped oxides as magnetic resonance imaging (MRI) contrasts will be confronted with other existing and researched MRI markers.

ZnO

Zinc oxide matrix exhibited phonon structure that allowed efficient luminescence when doped with foreign ions. Furthermore, those structures exhibited relatively efficient excitation and emission in the visible range, hence they were a perfect for various biomedical applications [274]. All those properties combined made them the first nanoparticles synthesized by our group by solvothermal method. The first route for synthesis of pure zinc oxide started with zinc chloride and zinc nitrate(V). Products exhibited very good crystallographic quality [275], but the stability issues prompted the further development of the method. Next, zinc oxide nanoparticles were synthesized using water or ethanol as solvent which impacted strongly on the defects in crystal lattice of the products [276]. As the control of the shape, size and crystalline quality were essential, further development was required. To improve the crystallinity of the product the mild thermal postprocessing was proposed [259]. This proved to be so efficient, that further development of zinc oxide nanoparticles included lanthanide and transition element doping. First, the syn-

thesis of magnetic ion doped ZnO was performed in ethylene glycol from acetate precursors [274]. It was shown that in case of the tested dopants, nanoparticles did not require additional postprocessing as they proved to have a pure ZnO phase. Then, in the search for luminescence in the visible range, various lanthanide ions were introduced into the matrix. Europium doped ZnO was found to be very sensitive to the conditions of the hydrothermal process, as both size of nanoparticles and defect distribution changed with pressure during synthesis [262]. Also, annealing of ZnO:Eu nanoparticles enhanced europium luminescence [259]. Furthermore, the ZnO-based nanoparticles were gradually degrading in aqueous suspension, a quality potentially of great importance for the bio-medical applications [81]. Finally, in ZnO:Eu nanoparticles it was found that aluminium addition had a strong influence over the shape and size of the product [270].

ZnAl$_2$O$_4$ (AZO)

Work on the microwave hydrothermal zinc aluminium spinel has started with doping of pure ZnO with 5-10% of aluminium [277]. The two synthesis methods were evaluated: hydrothermal in tubular reactor and microwave hydrothermal to verify which method would allow the direct formation of crystalline product. Nanoparticles prepared using periodic tubular microwave hydrothermal reactor exhibited very tiny average sizes of crystallites, around 2.2 nm [278]. As mentioned before this size-range was not suitable for biomedical applications. Thus work focused on the microwave hydrothermal stop-flow reactor, where addition of aluminium allowed better control of morphology and sizes of nanocrystals [279].

Both ZnO and AZO nanoparticles proved degradable in the biological media. For certain medical and research applications this property was considered extremely useful (*i.e.* monitoring of tumour progression with MRI or delivery of biologically-active substances through the gut barrier). However, for other applications, like fluorescence guided biopsy and surgery, the biostable (non-degradable) nanoparticle matrix seemed more suited.

Out of the wide bandgap, low phonon energy oxides, oxides of the elements from group 3 and 4 of periodic table were selected. They were insoluble in water, chemically resistant and biostable. Furthermore, they were well suited for doping with lanthanide ions. Finally, the bottom-up generation via microwave hydrothermal route was a method of choice for their synthesis. From those, the authors focused on two transition metal oxides: Zr and Y due to their confirmed long-term biocompatibility.

ZrO$_2$

Zirconium dioxide prepared using microwave hydrothermal technique was found fine-grained when compared to nanopowders prepared by calcination and formed crystalline lattices during synthesis [257]. TEM images of ZrO$_2$ presented in Figure 3 show nanoparticles prepared by precipitation calcination (Figure 3A) compared to (Figure 3B and C) fine and uniformly grained nanocrystals prepared by microwave hydrothermal treatment at 6 MPa. Pure microwave hydrothermally prepared ZrO$_2$ nanopowders were found to be sensitive to the partial pressure of surroundings [280]. Lanthanide ions were also investigated in ZrO$_2$ crystal lattice, to find various structural and spectroscopic mechanisms of luminescence in these materials. The most applicable dopants the authors designated for bio-medical applications were: Eu [281], Pr [260] and Tb [282]. Terbium doped nanoparticles were found to have density lower than bulk zirconia, indicating presence of hydroxide layer on the surface. Nanoparticles doped with low terbium concentrations were found to be stable in water suspension, and suitable for bioimaging in mice [258]. The microwaves driven hydrothermal method of production resulted in relatively small 2-10 nm nanoparticles (Figure 3C) of uniform size distribution (Figure 3D). This gave us a superb substrate for the further processing by thermal growth [257], which resulted with nanoparticles of narrow, tuneable size-distribution [272].

Y$_2$O$_3$

Microwave hydrothermal synthesis of Y$_2$O$_3$ started from nitrates(V) and resulted in crystallization of Y$_4$O(OH)$_9$(NO$_3$) phase, which had to be thermally postprocessed to obtain pure yttria [79]. Similar behaviour was found both for terbium and europium doped nanoparticles [269, 271]. During calcination an interesting phenomenon was observed. Inside the initial crystalline matrix, the recrystallisation process occurred, with tiny crystalline nodes similar in size and luminescent properties to quantum dots. As a result a packet of high-yield luminescent QDs within one large, biocompatible nanoparticle structure of the size well-matched to mentioned above processes of intracellular uptake and trafficking, was obtained. In Figure 4 transmission electron microscope (TEM) images shown the described phenomenon. In the first step Y$_4$O(OH)$_9$(NO$_3$) precursor crystals are grown with microwave hydrothermal method (Figure 4A). Then, after calcination at 400°C structure became non-uniform with visible nucleation seeds (Figure 4B). Following treatment at 800°C, nanocrystals of Y$_2$O$_3$ underwent recrystallization process with large,
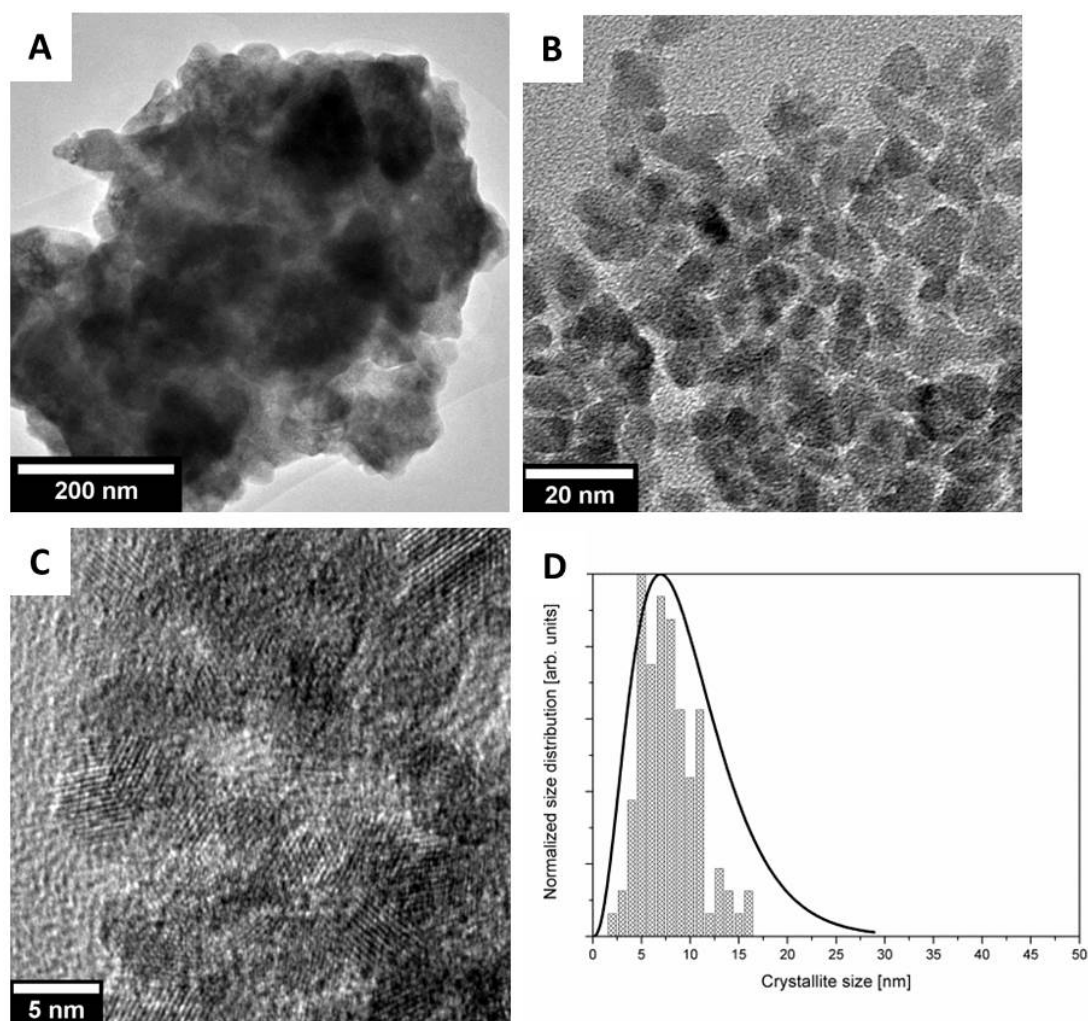
Figure 3: TEM images of ZrO_2 nanopowders prepared by (A) precipitation calcination method and (B) microwave hydrothermal process. Image (C) depicts ZrO_2:Tb nanoparticles. Panel (D) shows the grain size distribution of the final product as measured directly from TEM images and calculated using powder diffraction patterns

highly luminescent domains seen in Figure 4C. In the last step, at 1200°C yttrium oxide full filled the rods (Figure D).

3 Lanthanide-doped oxide nanoparticles for diagnostics of lung cancer – a proof of concept

Lung cancer is the most spread cancer in the world, of extremely heterogenous nature and origin. For the last few decades it was considered as one of the most deadly tumours, predominantly due to the frequency of metastases, difficulties in detection and treatment. Lung cancer is generally considered as the most common type of tumour in men. Int. Agency for Research on Cancer a part of World

Health Organization estimated that lung cancer was responsible for approximately 20% of cancer caused deaths in 2012 [1–3]. It is worth to emphasize that overall incidence ratio of this type of cancer to mortality is extremely high – 0.87. Likewise, regardless of rapid development in cancer diagnosis and therapy during last few decades, still a long-term survival rate of this destructive disease have barely improved over the last 50 years. According to annual report of American Cancer Society's (ACS) in 2017 the 5-year survival rate for both sexes is 18% and, separately, 15% for men and 21% for women [3].

3.1 Detection of lung cancer

As mentioned before, the most promising methods of cancer detection should be based on the pure physical
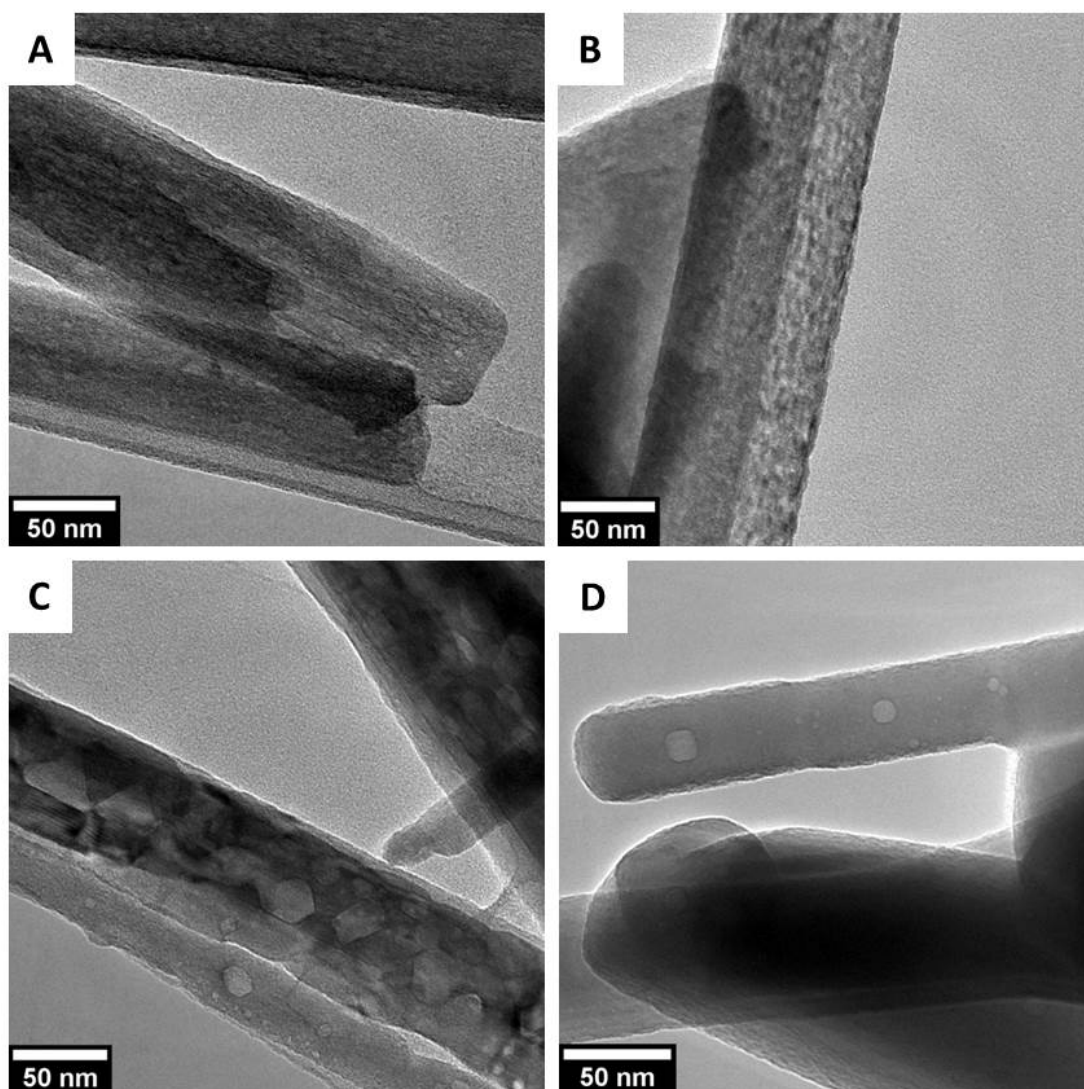
Figure 4: TEM images of Y_2O_3:Eu structures grown using microwave hydrothermal process (A) and additionally calcined at: 400°C (B), 800°C (C) and 1200°C (D)

properties of cancer microenvironment, namely the EPR effect. Enhanced permeabilization of tumour blood vessels combined with extremely poor lymph drainage facilitates the effective accumulation and prolonged retention of nanoparticles in the cancerous tissue.

The disadvantage of the method was that it did not allow to discriminate between the types and origin of the tumour. However, at the same time, this lack of specificity renders the method applicable for plethora of cancers, allowing their indiscriminate detection (Figure 1). Our research proved that specifically for the lung cancer the only nanoparticle permeability was observed in the cancer metastases which allowed a 100% selectivity of the proposed method of detection [272].

4 Multimodal markers

Nowadays, the search among scientific community focusses on the methods allowing effective detection of tumours during routine diagnostics with minimal or no side effects associated with the procedure. For this, the tumour specific biomarkers in bodily fluids, optical screening and magnetic resonance were designated as the most promising [283]. Unfortunately, at least for now, the biomarkers proved either highly non-specific, way to differentiate tumour disease from other inflammatory processes, or over-specific, able to detect only a very distinct type of cancer or even the single clone of cancer cells. The limitation of fluorescence or luminescence based contrasts is that in most of the cases it is not an in-situ method. The limited

penetration of both excitation and emission wavelengths results in the requirement of the surgical procedure with body penetration (*e.g.* laparoscopy). The only viable application of optical-based method are either fluorescence assisted surgery or biopsy, when the direct access to operation field is possible. Therefore, optical imaging was so challenging in the case of tumours located deep within the organs, that the only successful applications were the detection and treatment of skin melanomas and screening for potential breast cancers. Hereby, an approach either through the MRI method or combined, multimodal methods based on the magnetic and optical contrast is recommended. Those seem the most effective, and thus will be discussed below.

4.1 Contrasting agents for MRI

The contrasts for magnetic resonance imaging (MRI) were first used 25 years ago. Since then they were constantly developed. The first commercially available formulation was dimeglumine gadopentetate in 1988 (trade name Magnevist). Gadolinium has 7 free valence electrons and until recently, nearly all research focused on high potential of gadolinium as a contrasting agent [284]. Nowadays, a variety of contrasting agents for MRI are available, almost all based on different chelates of gadolinium (*i.e.* Gadobutrol, Gadoteridolum, Dimeglumine gadopentetate) [285–287]. All gadolinium-based contrast agents had a high magnetic moment. Therefore, their presence in the tissues effectively shortened the longitudinal relaxation time of hydrogen proton in water molecules, which provided a positive contrast, brightening the image of the T1 sequence [288].

Gadobutrol molecules have a macrocyclic structure, which proved more stable in the organisms than linear chelates. Macrocyclic chelates were gadolinium compounds associated with the lowest risk of nephrogenic fibrosis (NSF). Nephrogenic systemic fibrosis (NSF) was a rare and serious syndrome that could include fibrosis of the skin, joints, eyes, and internal organs. The first cases were identified in 1997, however its direct cause has not yet been determined. Nevertheless, studies indicated that NSF was associated with gadolinium exposure, at least in patients with a severe renal impairment [289].

The next heterocyclic compound used as a contrast agent was gadoteridol. This preparation caused enhanced contrast of the brain, spine, and surrounding tissues on the MRI images. It reduced the relaxation time T1 in the tissues where it accumulated. This was employed to visualize lesions, an abnormal blood flow through the vessels

or a compromise of the blood-brain-barrier. Furthermore, all those properties render it invaluable in the diagnostics of cancer and abscesses of the nerve tissue [290].

Dimeglumine gadopentetate was one of the oldest and least advanced gadolinium chelates. This compound was characterized by a linear molecular structure causing weaker bond of gadolinium ion, which could easily be substituted by zinc ion and released into the body. The release of gadolinium ions into the blood was low due to the rapid renal clearance of the drug, however it was not considered to be safe. Despite the general instability, linear chelates had some advantages: recent studies have shown that linear forms of chelates were less allergenic than macrocyclic structures [291].

Gadolinium derivatives were undoubtedly effective contrast agents, but they still had some serious drawbacks and limitations. The most serious problem was the strong toxicity of their primary contrasting ingredient – gadolinium ions. The chelated gadolinium ions did not show the acute toxicity, however free gadolinium ions accumulated in the liver, spleen and bones. There, they could cause a lethal effect, even at very low doses, with LD50 determined for mice at 0.2 mmol/kg [292, 293]. Concluding, the biosafety of contrast agents based on gadolinium was dependent on the *in vivo* tissue stability and high renal clearance of chelates [294, 295].

Successive generations of chelates had a greater number of carboxyl groups and more spatial structure. Molecules with a macrocyclic structure were strongly bound to gadolinium ions. This reduced ion releases and improved the safety of the formulations, but was not able to stop the ion leakage completely, and did not solve the accumulation and toxicity problems [296, 297].

Specifically, the strong negative effects of repeating MRI studies conducted with contrast agents came under the scientific scrutiny over the last several years. In 2006, the first study combining gadolinium-based contrast agents with the development of NSF was published [298]. This rapport caused huge controversy in the scientific world. Quickly, the thesis has been confirmed by numerous toxicological and pharmacological studies on animal models [299–302].

Also, a recent discovery of gadolinium residues in patients with healthy kidneys came as a shock. Abnormalities in T1 dentin relaxation time and pallidus globulin in the brain have been reported in patients with who previously underwent multiple MRI studies with gadolinium contrasting agents [303, 304]. Even though recently researches confirmed their transfer through the blood-brain-barrier, no specific data on how gadolinium-based contrast agents may have affected the central nervous sys-

tem [305]. Aforementioned risks associated with the use of well-established gadolinium ions, prompted studies on the alternatives. One of the candidates with T1-contrasting properties was a contrast based on the divalent manganese ion. Here, five free electrons resulted in reducing the T1 relaxation time, however not to the level of Gd. Two categories of contrast media based on this ion were proposed: small molecular and nanoparticle based contrasts. Small molecular factors were in their essentials similar to gadolinium contrasts with Mg ion replacing Gd in the chelates (*i.e.* Teslacan). For this injectable contrast agent the use of potassium manganate was approved for diagnostic use in 1997. However, in 2012, the manufacturer voluntarily resigned from admission to the European Union [306]. Manufacturer's decision has been caused by the severe negative aspects relater with the use of manganese ions. Like gadolinium, it was difficult to produce stable complexes and manganese ions were be displaced from the chelates. Released manganese ion was then passing through the calcium channel in the neurons with the risk of the brain damage [307]. Nowadays, manganese ions were recalled from the use as a contrast agents. The only potentially stable formulations regarding Mg ions were nanoparticles. Here to increase the amount of water molecules neighbouring the magnetic centres, nanoparticles were coated with high porosity silica. Such-prepared nanostructures had larger contact area which improved their relaxivity and potential contrasting properties [308].

A separate group of contrast agents were substances that affect the relaxation time of T2. They acted on the spin-spin interactions between hydrogen nuclei in water molecules which resulted as a negative contrast causing the T2 image to darken. One of the earliest and most common contrasting compounds active in the T2 were a variety of iron oxides, especially in the form of nanoparticles. The most important advantage of these nanoparticles was their relatively low toxicity, as iron in the oxides is present in their biological valency. However, there two serious problems in the applicability of iron oxides is the difficulty to distinguish them from the other iron-rich tissues [309, 310] and possibility to interact with general iron metabolism [311, 312]. Two iron oxides were considered particularly useful in medical applications: magnetite (Fe_3O_4) and its oxidized and more stable form of maghemite (γ-Fe_2O_3). To sustain superparamagnetic properties, the size of iron oxide nanoparticles could not exceed 1 nm for magnetite and 30 nm for maghemite. As an additional benefit, these nanomaterials did not show self-aggregation [313]. However, as mentioned before, these sizes promote the simple diffusion of nanopar-

ticles throughout the cell with huge problems in their elimination after procedure.

4.2 Core-shell and multimodal MRI contrasts

A breakthrough in the field of contrasting agents could be dual mode ultrasonic iron oxide nanocaps. They gave a positive contrast in sequences based on relaxation time T1 and negative in sequences T2. Unfortunately, their diameter was 3.3 ± 0.5 nm and all the tests were conducted in a specialized MRI apparatus with a power of 4.7 tesla [314]. A novelty in the field of T2 contrasting agents were the formulations utilizing Dy^{3+} ions either in the chelates or as nanoparticles. Due to the high magnetic moment, dysprosium exhibited excellent contrasting properties but only under a strong magnetic field (3-9 T). Yet again this proved to be a huge technical challenge, since only magnets between 1.5 and 3 tesla are generally used and considered safe for diagnostics. Generally, field strengths over 4.5 tesla were forbidden from medical use due to tissue overload and disturbance of ionic currents [315].

Another idea for nanoparticle-based MRI contrast was to combine two different materials in a single nanoparticle. Examples of such materials had a 15-nanometer-diameter core built from $MnFe_2O_4$ covered by a 1.5 nanometre-thick coat of $Gd_2O\,(CO_3)_2$. The outer layer had direct contact with the water molecules, which reduced the T1 relaxation time. The nucleus of the molecule induced local anomalies of the magnetic field, thus reducing the T2 relaxation time of the water molecules. Relationships between those two types of interaction could have been controlled by the thickness of the neutral SiO_2 insulating layer covering the whole structure. The use of heterogeneous nanostructures provided tremendous opportunities for modifying the properties of nanomaterials. However the kinetics of absorption, biodistribution and degradation/elimination of such materials require thorough evaluation and a holistic approach. It has been shown for various oxide-based nanostructures, it was difficult to predict how nanomaterials would behave in the living organism [78, 79, 81, 82, 272]. An example of such negligence was a study promoting nanoparticles of gadolinium oxide core, covered by zinc oxide insulating shell. The nanoparticles exhibited promising contrasting properties and their surfaces were easy to modify and claimed by authors to be biologically inert [316]. However, researchers failed to observe, that zinc oxide was biologically unstable, undergoing biodegradation whenever introduced into the tissues. Moreover, as it has been shown in our previous studies, ZnO nanoparticles were able to transfer through the blood-organ barriers,
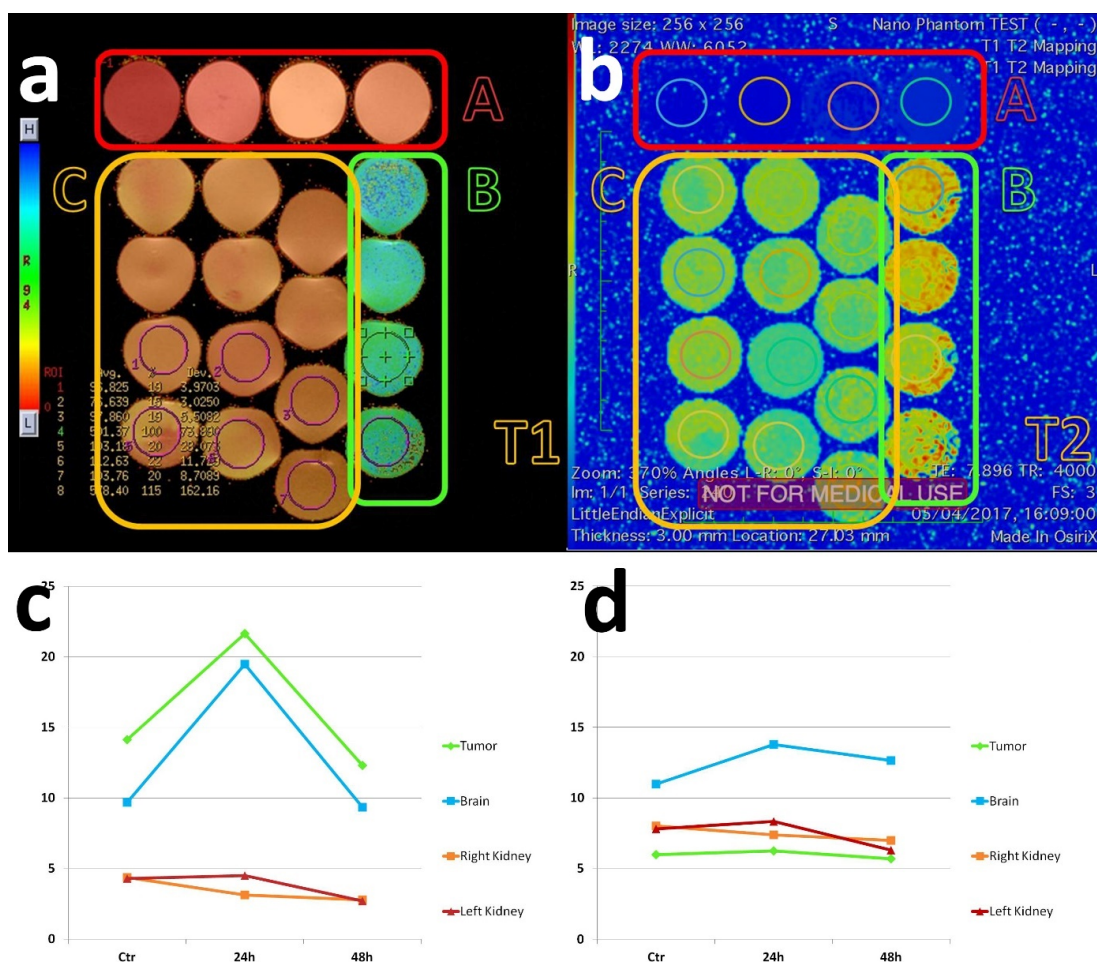
Figure 5: Agar gel phantoms in magnetic resonance (MR) imaging under T1 (a) and T2 (b) relaxation time. In both T1 and T2 relaxation time modalities the same materials were evaluated: (A) positive Gd-based commercial contrast at following concentrations (from left): 1, 2, 10, 28 mg/ml; (B) negative control probe (pure agar gel phantom); (C) experimental group with different types of nanoparticles (from the top): HfO_2:Fe, HfO_2:Gd, HfO_2:Eu and ZnO:Fe at concentrations (from the left): 1, 2, 10 mg/ml. Plots presented below reveal the average T2 relaxation time (expressed in relation to the lung tissue as a reference level) for the following tissues of rat patients of the veterinary oncology clinic: brain, left kidney, right kidney and cancer tissue, before administration of NPs, 24h after administration of NPs and 48 after administration of NPs. Age-related tumours developed in rats naturally and owners consent for the experimental diagnostic procedure was acquired. Two types of nanoparticles were evaluated: HfO_2:Gd (c) and HfO_2:Eu (d). For both nanoparticles the general tissue contrast was similar (compare results for brain and kidneys), with Gd-based contrast being more effective. Changes in the polarisation of contrast (positive vs. negative) in tumours reflected the different types of cancer, highly-vascularised for (c) and solid, low vascularised for (d)

including effective transport into the brain [81]. Thus, the proposed nanoparticles would not only allocate in the tissue highly affected by the toxicity of Gd, but also release gadolinium ions directly into the brain. As such, the suspected side-effects could be expected to be much higher than for traditional chelate-based formulations. Furthermore, in wurtzite type ZnO it is difficult to substitute zinc ions with trivalent lanthanides. The reasons are large difference in ionic radii of Zn^{2+} and Ln^{3+} (0.6 vs. 0.9 Å) as well as large difference in ions charges. In effect, there are different charge compensation mechanisms in ZnO crystals compared to ZrO_2. In zirconium dioxide Zr^{4+} ions are sub-

stituted by Ln^{3+} ions and the charge is compensated by formation of neutral oxygen vacancies. On the other hand, in ZnO compensation of Ln^{3+} presence in Zn^{2+} site is compensated by additional interstitial oxygen ions, which case is far less probable [322]. Even though, presence of the Eu^{3+} ions in ZnO lattice was confirmed by a few investigations of charge transfer phenomenon between dopant and oxygen ions [317], in majority cases it was shown that guest ions are not substituting zinc in the crystal lattice [319–322], but allocated on the surface of nanoparticle [262].

4.3 Biocompatible oxides for MRI and multimodal diagnostics

In this final chapter, a novel approach towards oxide-based contrasting agents for MRI and MRI-fluorescence would be presented. The three different approaches to create MRI-contrasting nanoparticles seem viable. First, the Gd ions of known contrasting properties in MRI need to be shielded from the contact with organism within the matrix of non-degradable nanoparticles. Secondly, a novel non-biodegrading nanoparticle could be constructed based on the magnetic properties of other 3+ lanthanides. Finally, the ions of known contrasting properties in the magnetic resonance (like Fe^{3+} or Ln^{3+}) could be embedded in the biodegradable nanoparticle to promote faster bioelimination of contrast.

For the first approach either the zirconium or hafnium dioxides as a base for the nanoparticles are proposed. Since, Gd ions match well the lattice of both oxide crystals, there is a high probability that Gd will substitute either the Zr or Hf in the matrix, remaining out of direct contact with the cells. Furthermore, both types of NPs were proven to be biostable. However, both ZrO_2 and HfO_2 nanoparticles have much longer clearance time from the tissues and both transfer through the brain tissue, the potential exposure to Gd will be relatively long. Moreover, the enhanced study regarding precise retention times and elimination kinetics from different tissues need to be conducted to evaluate the overall risks of proposed approach.

Secondly, in the same matrices the ions of confirmed biosafety can be embedded, *i.e.* Eu^{3+}. This, in increased content, exhibits both magnetic and fluorescence contrasts, enhancing the use of proposed formulation from MRI to the fluorescence-enhanced biopsy and surgery. This approach, however, has one limitation, for now those NPs proved to give magnetic contrast predominantly in the T2 relaxation time (Figure 5). Finally, nanoparticles composed of the biodegradable matrix doped with either aforementioned Eu^{3+} or Fe^{3+} ions, which exhibited promising results, if predominantly in the less specific contrast of T2, are proposed. Still, for the Fe doped nanoparticles, especially biodegradable ones, the impact of Fe ions on the general iron metabolism needs to be closely monitored.

For now, it can be showed the confirmed accumulation of ZrO_2:Eu and HfO_2:Gd nanoparticles in the liver 3h after IG in the experimental animals and negative T2 contrast in the tumours of rats surgically treated for tumours in the veterinary oncology clinic.

5 Summary

The present review concentrates on new, highly promising nano-materials and their development strategies. It is focussed on the multimodality of nanoparticles easily achievable in the oxide materials, and the early cancer detection combined with following fluorescence enhanced biopsy or surgery. Wide-band gap oxide materials, as discussed above, seem a good base material for the future medical applications, both in diagnostic and in therapy, and indeed in both (in the case of their multimodality). also It is also pointed out, that before a wider use of any new method for biomedical purposes, more information on safety aspects is required. Variety of fluorescent (or similar) markers investigated till now will never be allowed for medical applications use due to their intrinsic or long-term toxicity. Most of the studies in this area omits the critical issues of organism safety, prevelance of nanomaterials in the organism and the environmental impact of their application. Unfortunately, majority of work nowadays is done on cancer cell lines, with total disregard to even the primary cell line studies. As such most of them would never even go over the "interesting publication" level (*i.e.* heavy-metal based nanoparticles or graphene based strategies). Hereby, the authors strongly encourage the holistic approach, based on the animal models, with combination of base and applicable research of nanoparticle biosafety and routes of entry and elimination from the organism. This review also presents the initial studies into the development of Gd-devoid MRI contrasts, which could eliminate Gd-induced toxicity from this very promising non-invasive method of cancer diagnosis.

Finally, in the context of potential cancer detection/diagnostic, it is showed that oxide nanomaterials were able to transfer through the intact intestinal barrier and other organ barriers (like the highly impermeable blood-brain-barrier). This opens a new much safer than injection method of nanoparticle entry to the organism. Finally, it has been demonstrated that oxide-based nanoparticles were deposited in the tumour site without any additional surface modifications a phenomenon linked with the physical properties of tumour tissue: enhanced permeation and retention mechanism. This has a huge advantage over any other directed deposition strategy, as it can potentially pinpoint any and every type of tumour, a highly seeked-out asset for cancer screening and detection. Combined with fluorescent doping, apllication of oxide nanoparticles can be further enhanced to fluorescence guided biopsy and fluorescence guided surgery in cancer diagnosis and therapy.

References

[1] WHO 2009 - Global health risks: mortality and burden of disease attributable to selected major risks, 2009, Geneva: World Health Organization.

[2] Ferlay J., Soerjomataram I., Ervik M., Dikshit R., Eser S., Mathers C., Rebelo M., Parkin D.M., Forman D., Bray F., Globocan 2012: Estimated Cancer Incidence, Mortality and Prevalence Worldwide in 2012 v1.0, IARC CancerBase No. 11., 2013, Lyon, France: Int. Agency for Research on Cancer.

[3] ACS 2017- American Cancer Society's, Cancer Facts & Figures 2017

[4] Ramanujam N., Fluorescence spectroscopy of neoplastic and non-neoplastic tissues, Neoplasia., 2000, 2, 89-117.

[5] Ramanujam N., Mitchell M.F., Mahadevan A., Warren S., Thomsen S., Silva E., et al., In vivo diagnosis of cervical intraepithelial neoplasia using 337-nm-excited laser-induced fluorescence, Proc. Nat. Acad. Sci. USA, 1994, 91, 10193-10197.

[6] Koenig F., McGovern F.J., Althausen A.F., Deutsch T.F., Schomacker K.T., Laser induced autofluorescence diagnosis of bladder cancer, J. Urology, 1996, 156, 1597-1601.

[7] Maeda H., Macromolecular therapeutics in cancer treatment: the EPR effect and beyond, J. Control Release, 2012, 164, 138-144.

[8] Wilhelm S., Taveres A.J., Dai Q., Ohta S., Audet J., Dvorak H.F., Chan W.C., Analysis of nanoparticle delivery to tumours, Nature Reviews Materials, 2016, 1, 16014.

[9] Mondal S.B., Gao S., Zhu N., Liang R., Gruev V., Achilefu S., Real-time fluorescence image-guided oncologic surgery, Adv. Cancer Res., 2014, 124, 171-211.

[10] Ismael R., Schwander H., Hendrix P., Fluorescent Dyes and Pigments, Ullmann's Encyclopedia of Industrial Chemistry, 2000, Wiley-VCH Verlag GmbH & Co. KGaA.

[11] Medinitz L., Tetsuo H., Uyeda Y., Goldman E.R., Mattoussi H. Quatum dot bioconjugates for imaging, labeling and sensing, Nature Mater., 2005, 4, 435-446.

[12] Qi L., Gao X., Emerging application of quantum dots for drug delivery and therapy, Expert Opinion Drug Deliv., 2008, 5(3), 263-267.

[13] Jamieson T., Bakhshi R., Petrova D., Pocock R., Imani M., Seifalian A.M., Biological applications of quantum dots, Biomaterials, 2007. 28. 4717-4732.

[14] Medenitz I.L., Mattousi H., Clapp A.R., Potential clinical applications of quantum dots, Int. J. Nanomed., 2008, 3(2), 151-167.

[15] Mazumder S., Dey R., Mitra M.K., Mukherjee S., Das G.C., Review: Biofunctionalized Quantum Dots in Biology and Medicine, J. Nanomaterials, 2009,35, 10.1155/2009/815734.

[16] Fang M., Peng C.W., Pang D.W., Li Y., Quantum Dots for Cancer Research: Current Status, Remaining Issues, and Future Perspectives, Cancer Biol. Med., 2012, 9, 151-163.

[17] Michalet X., Pinaud F.F., Bentolila L.A., Tsay J.M., Doose S., Li J.J., Sundaresan G., Wu A.M., Gambhir S.S., Weiss S., Quantum Dots for Live Cells, in Vivo Imaging, and Diagnostics, Science, 2005, 307(5709), 538-544.

[18] SPIE Photonics West 2014, Paul Selvin Hot Topics presentation: New Small Quantum Dots for Neuroscience, SPIE Newsroom, DOI:10.1117/2.3201403.17.

[19] Tokumasu F., Fairhurst R.M., Ostera G.R., Brittain N.J., Hwang J., Wellems T.E., Dvorak J.A., Band 3 modifications in Plasmodium falciparum-infected AA and CC erythrocytes assayed by autocorrelation analysis using quantum dots, J. Cell Science, 2005; 118, 1091-1098.

[20] Dahan M., Diffusion Dynamics of Glycine Receptors Revealed by Single-Quantum Dot Tracking Science, 2003, 302 (5644), 442-445.

[21] Howarth M., Liu W., Puthenveetil S., Zheng Y., Marshall L.F., Schmidt M.M., Wittrup K.D., Bawendi M.G., Ting A.Y., Monovalent, reduced-size quantum dots for imaging receptors on living cells, Nature Methods, 2008, 5(5), 397-399.

[22] Akerman M.E., Warren C.W. Chan, Laakkonen P., Bhatia S.N., Ruoslahti E., Nanocrystal targeting in vivo, Proceedings of the National Academy of Sciences, 2002, 99 (20), 12617-12621.

[23] Farlow J., Seo D., Broaders K.E., Taylor M.J., Gartner Z.J., Jun Y.W., Formation of targeted monovalent quantum dots by steric exclusion, Nature Methods, 2013, 10(12), 1203-1205.

[24] Dwarakanath S., Bruno J.G., Shastry A., Phillips T., John A., Kumar A., Stephenson L.D., Quantum dot-antibody and aptamer conjugates shift fluorescence upon binding bacteria, Biochemical and Biophysical Research Communications, 2004, 325(3), 739-743.

[25] Zherebetskyy D., Scheele M., Zhang Y., Bronstein N., Thompson C., Britt D., Salmeron M., Alivisatos P., Wang L.W., Hydroxylation of the surface of PbS nanocrystals passivated with oleic acid, Science, 2014, 344(6190), 1380-1384.

[26] Ballou B., Lagerholm B.C., Ernst L.A., Bruchez M.P., Waggoner A.S., Noninvasive Imaging of Quantum Dots in Mice, Bioconjugate Chemistry, 2004, 15(1), 79-86.

[27] Daou J.T., Li L., Reiss P., Josserand V., Texier I., Effect of Poly(ethylene glycol) Length on the in Vivo Behavior of Coated Quantum Dots, Langmuir, 2009, 25, 3040-3044.

[28] Hotz C.Z., Applications of Quantum Dots in Biology: An Overview, Rosenthal S.J., Wright D.W., NanoBiotechnology Protocols, Volume 2, Humana Press Inc., New Jersey, 2005, 1-18.

[29] Medarova Z., Pham W., Farrar C, Petkova V., Moore A., In vivo imaging of siRNA delivery and silencing in tumors, Nat. Med., 2007, 13, 372-377.

[30] McCarthy J.R., Kimberly A.K., Sun E.Y., Weissleder R., Targeted delivery of multifunctional magnetic nanoparticles, Nanomed., 2007, 2, 153-167.

[31] Harisinghani M.G., Barentsz J., Hahn P.F., Deserno W.M., Tabatabaei S., Hulsbergen van de Kaa C., de la Rosette J., Weissleder R., Noninvasive detection of clinically occult lymph-node metastases in prostate cancer, N. Engl. J. Med., 2003, 348, 2491-2499.

[32] Rhyner M., Smith A., Gao X., Nie S., Quantum dots and multifunctional nanoparticles: new contrast agents for tumor imaging, Nanomedicine (Lond), 2006, 1, 209-217.

[33] Xing Y., Chaudry Q., Shen C., Kong K.Y., Zhau H.E., Chyng L.W., Petros J.A., O'Regan R.M., Yezhelyev M.V., Simons J.W., Wang M.D., Nie S., Bioconjugated quantum dots for multiplexed and quantitative immunohistochemistry, Nat. Protoc., 2007, 2, 1152-1165.

[34] Wu X., Liu H., Liu J., Haley K.N., Treradway J.A., Larson J.P., Ge N., Peale F., Bruchez M.P., Immunofluorescent labeling of can-

cer marker Her2 and other cellular targets with semiconductor quantum dots, Nat. Biotechnol., 2003, 21, 41-46.

[35] Kim S., Lim Y.T., Soltesz E.G., De Grand A.M., Lee J., Nakayama A., Parker J.A., Mihaljevic T., Laurence R.G., Dor D.M., Cohn L.H., Bawendi M.G., Frangioni J.V., Near-infrared fluorescent type II quantum dots for sentinel lymph node mapping, Nat. Biotechnol., 2004, 22, 93-97.

[36] Chan W.C., Nie S., Quantum dot bioconjugates for ultrasensitive nonisotopic detection, Science, 1998, 281, 2016-2018.

[37] Bruchez M. Jr., Moronne M., Gin P., Weiss S., Alivisatos A.P., Semiconductor nanocrystals as fluorescent biological labels, Science, 1998, 281, 2013-2016.

[38] Gao X., Cui Y., Levenson R.M., Nie S., In vivo cancer targeting and imaging with semiconductor quantum dots, Nat. Biotechnol., 2004, 22, 969-976.

[39] Tada H., Higuchi H., Wanatabe T.M., Ohuchi N., In vivo real-time tracking of single quantum dots conjugated with monoclonal anti-HER2 antibody in tumors of mice, Cancer Res., 2007, 67, 1138-1144.

[40] Zhang H., Sachdev D., Wang C., Hubel A., Gaillard-Kelly M., Yee D., Detection and downregulation of type I IGF receptor expression by antibodyconjugated quantum dots in breast cancer cells, Breast Cancer Res. Treat., 2009, 114, 277-285.

[41] Yong K.T., Ding H., Roy I., Law W.C., Bergey E.J., Maitra A., Prasad P.N., Imaging pancreatic cancer using bioconjugated InP quantum dots, ACS Nano, 2009, 3, 502-510.

[42] Voura E.B., Jaiswal J.K., Mattoussi H., Simon S., Tracking metastatic tumor cell extravasation with quantum dot nanocrystals and fluorescence emission-scanning microscopy, Nat. Med., 2004, 10, 993-998.

[43] Cai W., Shin D.W., Chen K., Gheysens O., Cao Q., Wang S.X., Gambhir S.S., Chen X., Peptide-labeled near-infrared quantum dots for imaging tumor vasculature in living subjects, Nano Lett., 2006, 6, 669-676.

[44] Stroh M., Zimmer J.P., Duda D.G., Levchenko T.S., Cohen K.S., Brown E.B., Scadden D.T., Torchilin V.P., Bawendi M.G., Fukumura D., Jain R.K., Quantum dots spectrally distinguish multiple species within the tumor milieu in vivo, Nat. Med., 2005, 11, 678-682.

[45] Li Z., Wang K., Tan W., Li J., Fu Z., Ma C., Li H., He X., Liu J., Immunofluorescent labeling of cancer cells with quantum dots synthesized in aqueous solution, Anal. Biochem., 2006, 354, 169-174.

[46] Dubertret B., Skourides P., Norris D.J., Noireaux V., Brivanlou A.H., Libchaber A., In vivo imaging of quantum dots encapsulated in phospholipid micelles, Science, 2002, 298, 1759-1762.

[47] Smith J.D., Fisher G.W., Waggoner A.S., Campbell P.G., The use of quantum dots for analysis of chick CAM vasculature, Microvasc. Res., 2007, 73, 75-83.

[48] Zimmer J.P., Kim S.W., Ohnishi S., Tanaka E., Frangioni J.V., Bawendi M.G., Size series of small indium arsenide-zinc selenide core-shell nanocrystals and their application to in vivo imaging, J. Am. Chem. Soc., 2006, 128, 2526-2527.

[49] Kim S.W., Zimmer J.P., Ohnishi S., Tracy J.B., Frangioni J.V., Bawendi M.G., Engineering InAs(x)P(1-x)/InP/ZnSe III-V alloyed core/shell quantum dots for the nearinfrared, J. Am. Chem. Soc., 2005, 127, 10526-10532.

[50] Thorne R.G., Nicholson C., In vivo diffusion analysis with quantum dots and dextrans predicts the width of brain extracellular space, Proc. Natl. Acad. Sci. U S A ,2006, 103, 5567-5572.

[51] Neuhauser R.G., Shimizu K.T., Woo W.K., Empedocles S.A., Bawendy M.G., Correlation between Xuorescence intermittency and spectral diVusion in single semiconductor quantum dots, Phys. Rev. Lett., 2000, 85, 3301-3304.

[52] Eiha N., Maenosono S., Hanaki K., Yamamoto K., Yamaguchi Y., Collective Xuorescence oscillation in a water dispersion of colloidal quantum dots, Jpn. J. Appl. Phys., 2003, 42, 310-313.

[53] Uematsu T., Kimura J., Yamaguchi Y., The reversible photoluminescence enhancement of a CdSe/ZnS nanocrystal thin Wlm, Nanotechnol., 2004, 15, 822-827.

[54] Kimura J., Uematsu T., Maenosono S., Yamaguchi Y., Photoinduced Xuorescence enhancement in CdSe/ZnS quantum dot submonolayers sandwiched between insulating layers: inXuence of dot proximity, J. Phys. Chem. B, 2004, 108, 13258-13264.

[55] Tang J., Marcus R.A., Mechanisms of Fluorescence blinking in semiconductor nanocrystal quantum dots, J. Chem. Phys., 2005, 123, 054704.

[56] Yao J., Larson D.R., Vishwasrao H.D., Zipfel W.R., Webb W.W., Blinking and nonradiant dark fraction of water-soluble quantum dots in aqueous solution, Proc. Natl. Acad. Sci., 2005, 102, 14284-14289.

[57] Marchuk K., Guo Y., Sun W., Vela J., Fang N., High-Precision Tracking with Non-blinking Quantum Dots Resolves Nanoscale Vertical Displacement, J. Amer. Chem. Soc., 2012, 134(14), 6108-11.

[58] Lane L.A., Smith A.M., Lian T., Nie S., Compact and Blinking-Suppressed Quantum Dots for Single-Particle Tracking in Live Cells, The J. Physical Chemistry B., 2014, 118(49), 14140-14147.

[59] Vela J., Htoon H., Chen Y., Park Y.S., Ghosh Y., Goodwin P.M., Werner J.H., Wells N.P., Casson J.L., Hollingsworth J.A., Effect of shell thickness and composition on blinking suppression and the blinking mechanism in "giant" CdSe/CdS nanocrystal quantum dots, J. Biophotonics, 2010. 3(10-11), 706-717.

[60] Colvin V.L., The potential environmental impact of engineered nanomaterials, Nature Biotechnol., 2003, 21, 1166-1170.

[61] Hoet P.H., Bruske-Hohlfeld I., Salata O.V., Nanoparticles - known and unknown health risks, J. Nanobiotechnol., 2004, 2, 2-12.

[62] Pelley J.L., Daar A.S., Saner M.A., State of Academic Knowledge on Toxicity and Biological Fate of Quantum Dots, Toxicol. Sci., 2009, 112(2), 276-96.

[63] Derfus A.M., Chan W.C.W., Bhatia S.N., Probing the Cytotoxicity of Semiconductor Quantum Dots, Nano Lett., 2004, 4(1), 11-18.

[64] Liu W., Zhang S., Wang L., Qu C., Zhang C., Hong L., Yuan L., Huang Z., Wang Z., Liu S., Jiang G., CdSe Quantum Dot (QD)-Induced Morphological and Functional Impairments to Liver in Mice, PLoS ONE, 2011, 6(9), e24406.

[65] Hillyer J.F., Albrecht R.M., Gastrointestinal persorption and tissue distribution of differently sized colloidal gold nanoparticles, J. Pharm. Sci., 2001, 90(12), 1927-1936.

[66] Green M., Howman E., Semiconductor quantum dots and free radical induced DNA nicking, Chem. Commun., 2005, (1), 121.

[67] Hardman R.A., Toxicologic Review of Quantum Dots: Toxicity Depends on Physicochemical and Environmental Factors, Environ. Health Perspect., 2006, 114(2), 165-172.

[68] Rzigalinski B.A., Strobl J.S., Cadmium-Containing Nanoparticles: Perspectives on Pharmacology & Toxicology of Quantum Dots, Toxicol. Appl. Pharmacol., 2009, 238(3), 280-288.

[69] Hoshino A., Hanada S., Yamamoto K., Toxicity of nanocrystal quantum dots: the relevance of surface modifications, Arch. Toxicol., 2011, 85, 707-720.

[70] Landin L., Miller M.S., Pistol M., Pryor C.E., Samuelson L., Optical studies of individual InAs quantum dots in GaAs: few-particle effects, Science, 1998, 280, 262-264.

[71] Pradhan N., Battaglia D.M., Liu Y., Peng X., Efficient, stable, small, and water-soluble doped ZnSe nanocrystal emitters as non-cadmium biomedical labels, Nano Lett., 2007, 7, 312-317.

[72] Takeuchi I., Nobata S., Oiri N., Tomoda K., Makino K., Biodistribution and excretion of colloidal gold nanoparticles after intravenous injection: Effects of particle size, Biomed. Mater. Eng., 2017, 28(3), 315-323.

[73] Yang L., Kuang H., Zhang W., Aguilar Z.P., Wei H., Xu H., Comparisons of the biodistribution and toxicological examinations after repeated intravenous administration of silver and gold nanoparticles in mice, Sci. Rep., 2017, 7(3303).

[74] Sonavane G., Tomoda K., Makino K., Biodistribution of colloidal gold nanoparticles after intravenous administration: Effect of particle size, Colloids Surf. B: Biointerfaces, 2008, 66, 274-280.

[75] Akerman M.E., Chan W.C.W., Laakkonen P., Bhatia S.N., Ruosiahti E., Nanocrystal targeting in vivo, PNAS, 2002, 99(20), 12617-12621.

[76] Soares D.C., Ferreira T.H., de Ferreira C.A., Cardoso V.N., de Sousa E.M., Boron nitride nanotubes radiolabeled with 99mTc: Preparation, physicochemical characterization, biodistribution study, and scintigraphic imaging in Swiss mice, Int. J. Pharmaceutics, 2011, 423(2), 489-495.

[77] Volkheimer G.Z., The Phenonenon of persorption - history and facts. in: Absorption of orally administered enzymes, Ed.: Gardner MLG i Steffens KJ, Springer-Verlag Berlin Heidelberg 1995, Germany, 1993, 87(3), 217-221.

[78] Godlewski M.M., Godlewski M., Superradiant rare-earth doped nanocrystals in the study of persorption processes in the adult intestine, In: Méndez-Vilas A, editor. Current Microscopy Contributions to Adv. Sci. Technol., Spain: Formatex, 2012, p. 582-90.

[79] Godlewski M.M., Kaszewski J., Szal A., Slonska A., Domino M.A., Mijowska E., Witkowski B.S., Godlewski M., Size of nanocrystals affects their alimentary absorption in adult mice, Veterinary Med., 2014, 70, 558-563.

[80] Slonska A., Kaszewski J., Wolska-Kornio E., Witkowski B., Wachnicki L., Mijowska E., Karakitsou V., Gajewski Z., Godlewski M., Godlewski M.M., Luminescent properties of ZrO_2:Tb nanoparticles for applications in neuroscience, Optical Mater., 2016, 59, 96-102.

[81] Kielbik P., Kaszewski J., Wolska E., Gralak M.A., Godlewski M., Godlewski M.M., Biodegradation of the ZnO:Eu nanoparticles in the tissues of adult mouse after alimentary application, Nanomed.: Nanotechnol., Biol. Med., 2017, 13, 843-852.

[82] Kielbik P., Kaszewski J., Godlewski M., Godlewski M.M., Cytometric analysis of Zn-based nanoparticles for biomedical applications, In: Microscopy and imaging science: practical approaches to applied research and education, Microscopy Book Series #7, Ed: A. Mendez-Vilas. Formatex, Spain, Series #7, 2017, 89-96.

[83] Godlewski M., Leskela M., Excitation and recombination processes during electroluminescence of rare earth-activated materials, Critical Rev. Solid State Mater. Sci., 1994, 19(4), 199-239.

[84] Dieke G.H., Spectra and Energy Levels of Rare Earth Ions in Crystals, Interscience Publishers, New York, 1968.

[85] Goldberg M.C., Weiner E.R., Luminescence Applications, ACS Symposium Series, American Chemical Society, Washington, DC, 1989.

[86] Gahlmann A., Moerner W.E., Exploring bacterial cell biology with single-molecule tracking and super-resolution imaging, Nature Reviews Microbiology, 2014, 12, 9-22.

[87] You Y., Park S.Y., Phosphorescent iridium(III) complexes: toward high phosphorescence quantum efficiency through ligand control, Dalton Trans., 2009, 1267-1282.

[88] Zhao Q., Liu Sh., Shi M., Wang Ch., Yu M., Li L., Li F., Yi T., Huang Ch., Series of New Cationic Iridium(III) Complexes with Tunable Emission Wavelength and Excited State Properties: Structures, Theoretical Calculations, and Photophysical and Electrochemical Properties, Inorg. Chem., 2006, 45, 6152-6160.

[89] Berggren K., Chernokalskaya E., Steinberg T.H., Kemper C., Lopez M.F,. Diwu Z., Haugland R.P., Patton W.F., Background-free, high sensitivity staining of proteins in one- and two-dimensional sodium dodecyl sulfate-polyacrylamide gels using a luminescent ruthenium complex, Electrophoresis, 2000, 21, 2509-2521.

[90] Tang F., Wang Ch., Wang J., Wang X., Li L., Organic-inorganic hybrid nanoparticles with enhanced fluorescence, Colloids Surf. A: Physicochem. Eng. Aspects, 2015, 480, 38-44.

[91] Bastakoti B.P., Hsu Y.C., Liao S.H., Wu K.C., Inoue M., Yusa S., Nakashima K., Yamauchi Y., Inorganic-organic hybrid nanoparticles with biocompatible calcium phosphate thin shells for fluorescence enhancement, Chem. Asian. J., 2013, 8(6), 1301-5.

[92] Vivero-Escoto J.L., Huang Y.T., Inorganic-Organic Hybrid Nanomaterials for Therapeutic and Diagnostic Imaging Applications, Int. J. Mol. Sci., 2011, 12(6), 3888-3927.

[93] Kumar B., Jalodia K., Kumar P., Gautam H.K., Recent Adv. nanoparticle-mediated drug delivery, J. Drug Deliv. Sci. Technol., 2017, 41, 260-268.

[94] Lucky S.S., Khee Soo Ch., Zhang Y., Nanoparticles in Photodynamic Therapy, Chem. Rev., 2015, 115, 1990-2042.

[95] Sharma P., Brown S., Walter G., Santra S., Moudgil B., Nanoparticles for bioimaging, Adv. Colloid and Interf. Sci., 2006, 123-126, 471-485. 026

[96] Nune S.K., Gunda P., Thallapally P.K., Lin Y-Y., Forrest M.L., Berkland C.J., Nanoparticles for biomedical imaging, Expert Opin. Drug. Deliv., 2009, 6(11), 1175-1194.

[97] Wolfbeis O.S., An overview of nanoparticles commonly used in fluorescent bioimaging, Chem. Soc. Rev., 2015, 44, 4743.

[98] Chen M., Yin M., Design and development of fluorescent nanostructures for bioimaging, Progr. Polymer Sci., 2014, 39, 365-395.

[99] Li Z., Sun Q., Zhu Y., Tan B., Xu Z.P., Shi S.X., Ultra-small fluorescent inorganic nanoparticles for bioimaging, J. Mater. Chem. B., 2014, 2, 2793.

[100] Peng Z., Han X., Li Sh., Al-Youbi A.O., Bashammakh A.S., El-Shahawi M.S., Leblanc R.M., Carbon dots: Biomacromolecule interaction, bioimaging and nanomedicine, Coord. Chem. Rev., 2017, 343, 256-277.

[101] Lin J., Chen X., Huang P., Graphene-based nanomaterials for bioimaging, Adv. Drug Deliv. Rev., 2016, 105, 242-254.

[102] Zang Z., Zeng X., Wang M., Hu W., Liu C., Tang X., Tunable photoluminescence of water-soluble AgInZnS-grapheneoxide (GO) nanocomposites and their application in-vivo bioimaging, Sensors and Actuators B, 2017, 252, 1179-1186.

[103] Lovric J., Bazzi H.S., Cuie Y., Fortin G.R.A., Winnik F.M., Maysinger D., Differences in subcellular distribution and toxicity of green and red emitting CdTe quantum dots, J. Mol. Med., 2005, 83(5), 377-385.

[104] Wang L., Nagesha D.K., Selvarasah S., Dokmeci M.R., Carrier R.L., Toxicity of CdSe Nanoparticles in Caco-2 Cell Cultures, J.

Nanobiotechnol., 2008, 6, 11.

[105] Pan Y., Neuss S., Leifert A., Fischler M., Wen F., Simon U., Schmid G., Brandau W., Jahnen-Dechent W., Size-dependent cytotoxicity of gold nanoparticles, Small, 2007, 3(11), 1941-1949.

[106] Cho W.S., Cho M., Jeong J., Choi M., Cho H.Y., Han B.S., Kim S.H., Kim O.H., Lim Y.T., Chung B.H., Jeong J., Acute toxicity and pharmacokinetics of 13 nm-sized PEG-coated gold nanoparticles, Toxicol. Appl. Pharmacol., 2009, 236, 16-24.

[107] Vasyukova I., Gusev A., Tkachev A., Reproductive toxicity of carbon nanomaterials: a review, Nanobiotech 2015. IOP Conf. Series: Mater. Sci. Eng., 2015, 98, 012001.

[108] Kobayashi N., Izumi H., Morimoto Y., Review of toxicity studies of carbon nanotubes, J. Occup. Health, 2017, 59(5), 394-407.

[109] Firme C.P., Bandaru P.R., Toxicity issues in the application of carbon nanotubes to biological systems, Nanomed.: Nanotechnol., Biol. Med., 2010, 6(2), 245-256.

[110] Franken P.A., Weinreich G., Peters C.W., Weinreich G., Generation of optical harmonics, Phys. Rev. Lett., 1961, 7. 118-119.

[111] Bloembergen N.. Solid State Infrared Quantum Counters. Phys. Rev. Lett., 1959, 2, 84.

[112] Auzel F., Compteur quantique par transfert d'energie entre deux ions de terres rares dans un tungstate mixte et dans un verre, C. R. Acad. Sci., Paris, 1966, 262, 1016-1019.

[113] Auzel F., Upconversion and Anti-Stokes Processes with f and d Ions in Solids, Chem. Rev., 2004, 104 (1), 139-174.

[114] Zhou J., Liu Q., Feng W., Sun Y., Li F., Upconversion Luminescent Materials: Advances and Applications, Chem. Rev., 2015, 115, 395-465.

[115] Abbasa M., Siddiqia M.H., Khana K., Zahrab K., Naqvi A.U.N., Haematological evaluation of sodium fluoride toxicity in oryctolagus cuniculus, Toxicol. Rep., 2017, 4, 450-454.

[116] Camargo J.A., Fluoride toxicity to aquatic organisms: a review, Chemosphere, 2003, 50, 251-264.

[117] Reinhard C.H., Valiente R., Gudel H.U., Exchange-Induced Upconversion in Rb_2MnCl_4:Yb^{3+}, J. Phys. Chem. B, 2002, 106, 10051-10057.

[118] Beurer E., Grimm J., Gerner P., Gudel H.U., New Type of Near-Infrared to Visible Photon Upconversion in Tm^{2+}-Doped $CsCaI_3$, J. Am. Chem. Soc., 2006, 128, 3110-3111.

[119] Mader H.S., Kele P., Saleh S.M., Wolfbeis O.S., Upconverting luminescent nanoparticles for use in bioconjugation and bioimaging, Curr. Opinion Chem. Biol., 2010, 14, 582-596.

[120] Xiao L., Wang R., Sun Z., Chen Y., Zhao E., Liu L., Enhanced red upconversion emission of Er^{3+}-doped ZnO by post-annealing, J. Luminescence, 2017, 192, 668-674.

[121] Yi G., Peng Y., Gao Z., Strong Red-Emitting near-Infrared-to-Visible Upconversion Fluorescent Nanoparticles, Chem. Mater., 2011, 23, 2729-2734.

[122] Vetrone F., Boyer J.C.H., Capobianco J.A., Speghini A., Bettinelli M., NIR to Visible Upconversion in Nanocrystalline and Bulk Lu_2O_3:Er^{3+}, J. Phys. Chem. B, 2002, 106, 5622-5628.

[123] Patra A., Friend Ch.S., Kapoor R., Prasad P.N., Fluorescence Upconversion Properties of Er^{3+}-Doped TiO_2 and $BaTiO_3$ Nanocrystallites, Chem. Mater., 2003, 15, 3650-3655.

[124] Vetrone F., Boyer J.C.H., Capobianco J.A., Speghini A., Bettinelli M., Luminescence Spectroscopy and Near-Infrared to Visible Upconversion of Nanocrystalline $Gd_3Ga_5O_{12}$:Er^{3+}, J. Phys. Chem. B, 2003, 107, 10747-10752.

[125] Taniguchi T., Murakami T., Funatsu A., Hatakeyama K., Koinuma M., Matsumoto Y., Reversibly Tunable Upconversion Lumines-

cence by Host-Guest Chemistry, Inorg. Chem., 2014, 53, 9151-9155.

[126] Syamchand S.S., Sony G., Europium enabled luminescent nanoparticles for biomedical applications, J. Luminescence, 2015, 165, 190-215.

[127] Jayadevan K.P., Tseng T.Y., Oxide nanoparticles, Encyclopedia of Nanoscience and Nanotechnology, 2004, 337-376.

[128] Hannink R.H.J., Hill A.J. (ed.), Nanostructure control of materials, Woodhead Publishing Limited, 2006.

[129] Gogotsi Y. (ed.), Nanomaterials handbook, CRC Press, 2006.

[130] Lakshmanan A. (ed.). Sintering of ceramics, InTech, 2012.

[131] Dong H., Du S.R., Zheng X.Y., Lyu G.M., Sun L.D., Li L.D., Zhang P.Z., Zhang C., Yan C.H, Lanthanide Nanoparticles: From Design toward Bioimaging and Therapy, Chem. Rev., 2015, 115, 10725-10815.

[132] Kim J.H., Park K., Nam H.Y., Lee S., Kim K., Kwon I.C., Polymers for bioimaging, Prog. Polym. Sci., 2007, 32, 1031-1053.

[133] Han G.M., Li H., Huang X.X., Kong D.M., Simple synthesis of carboxyl-functionalized upconversion nanoparticles for biosensing and bioimaging applications, Talanta, 2016, 147, 207-12.

[134] Tsang M.K., Chan C.F., Wong K.L., Hao J., Comparative studies of upconversion luminescence characteristics and cell bioimaging based on one-step synthesized upconversion nanoparticles capped with different functional groups, J. Luminescence, 2015, 157, 172-178.

[135] Dong H., Du S.R., Zheng X.Y., Lyu G.M., Sun L.D., Li L.D., Zhang P.Z., Zhang C., Yan C.H., Lanthanide Nanoparticles: From Design toward Bioimaging and Therapy, Chem. Rev., 2015, 115, 10725-10815.

[136] Ronda C.R., Justel T., Nikol H., Rare earth phosphors: fundamentals and applications, J. All. Comp., 1998, 275-277, 669-676.

[137] Ronda C.R., Phosphors for lamps and displays: an applicational view, J. All. Comp., 1995, 225, 534-538.

[138] Dhand Ch., Dwivedi N., Loh X.J., Ying A.N.J., Verma N.K., Beuerman R.W., Lakshminarayanan R., Ramakrishna S., Methods and strategies for the synthesis of diversenanoparticles and their applications: a comprehensive overview, RSC Adv., 2015, 5, 105003.

[139] Swihart M.T., Vapor-phase synthesis of nanoparticles, Curr. Opinion Colloid Interf. Sci., 2003, 8, 127-133.

[140] Rajput N., Methods of preparation of nanoparticles - a review, Int. J. Adv. Eng. Technol., 2015, 7(4), 1806-1811.

[141] Iskandar F., Nanoparticle processing for optical applications - A review, Adv. Powder Technol., 2009, 20, 283-292.

[142] Wegner K., Walker B., Tsantilis S., Pratsinis S.E., Design of metal nanoparticle synthesis by vapor flow condensation, Chem. Eng. Sci., 2002, 57, 1753-62.

[143] Nanda K.K., Kruis F.E., Fissan H., Acet H., Band-gap tuning of PbS nanoparticles by in-flight sintering of size classified aerosols, J. Appl. Phys., 2002, 91, 2315-21.

[144] Marine W., Patrone L., Lukyanchuk B., Sentis M., Strategy of nanocluster and nanostructure synthesis by conventional pulsed laser ablation, Appl. Surf. Sci., 2000, 154-155, 345-52.

[145] Schmechel R., Kennedy M., von Seggern H., Winkler H., Kolbe M., Fischer R.A., Li X., Benker A., Winterer M., Hahn H., Luminescence properties of nanocrystalline Y_2O_3:Eu^{3+} in different host materials, J. Appl. Phys., 2001, 89, 1679-86.

[146] Chang W., Skandan G., Hahn H., Danforth S.C., Kear B.H., Chemical vapor condensation of nanostructured ceramic powders, Nanostructured Mater., 1994, 4(3), 345-351.

[147]   Weber A.P., Seipenbusch M., Kasper G., Application of aerosol techniques to study the catalytic formation of methane on gas-borne nickel nanoparticles, J. Phys. Chem. A, 2001, 105, 8958-63.

[148]   Borsella E., Botti S., Cesile M.C., Martelli S., Nesterenko A., Zappelli P.G., MoS_2 nanoparticles produced by laser induced synthesis from gaseous precursors, J. Mater. Sci. Lett., 2001, 20, 187-91.

[149]   Heberlein J., Postel O., Girshick S., McMurry P., Gerberich W., Iordanoglou D Di Fonzo F., Thermal plasma deposition of nanophase hard coatings, Surf. Coat. Technol. 2001, 142-144, 265-71.

[150]   Janzen C., Roth P., Formation of Fe_2O_3 nano-particles in doped low-pressure H_2 /O_2 /Ar flames, Combust Flame, 2001, 125, 1150-61.

[151]   Sarigiannis D., Peck J.D., Kioseoglou G., Petrou A., Mountziaris T.J., Characterization of vapor-phase-grown ZnSe nanoparticles, Appl. Phys. Lett., 2002, 80, 4024-6.

[152]   Biskos G., Vons V., Yurteri C.U., Schmidt-Ott A., Generation and Sizing of Particles for Aerosol-Based Nanotechnology, KONA Powder and Particle J., 2008, 26, 13-35.

[153]   Teoh W.Y., A Perspective on the Flame Spray Synthesis of Photocatalyst Nanoparticles, Materials, 2013, 6, 3194-3212.

[154]   Okuyama K., Lenggoro I.W., Preparation of nanoparticles via spray route, Chem. Eng. Sci., 2003, 58, 537-547.

[155]   Stunda-Zujeva A., Irbe Z., Berzina-Cimdina L., Controlling the morphology of ceramic and composite powders obtained via spray drying - A review, Ceram. Int., 2017, 43, 11543-11551.

[156]   Abdelwahed W., Degobert G., Stainmesse S., Fessi H., Freeze-drying of nanoparticles: Formulation, process and storage considerations, Adv. Drug Deliv. Rev., 2006, 58, 1688-1713.

[157]   Bang J.H., Suslick K.S., Applications of Ultrasound to the Synthesis of Nanostructured Materials, Adv. Mater., 2010, 22, 1039-1059.

[158]   Kohno M., Mokudai T., Ozawa T., Niwano Y., Free radical formation from sonolysis of water in the presence of different gases, J. Clin. Biochem. Nutr., 2011, 49(2), 96-101.

[159]   Wood R.J., Lee J., Bussemaker A.J., A parametric review of sonochemistry: Control and augmentation of sonochemical activity in aqueous solutions, Ultrason. Sonochem., 2017, 38, 351-370

[160]   Pokhrel N., Vabbina P.K., Pala N., Sonochemistry: Science and Engineering, Ultrason. Sonochem., 2016, 29, 104-128.

[161]   Gonzalez-Garcia J., Esclapez M.D., Bonete P., Hernandez Y.V., Garreton L.G., Saez V., Current topics on sonoelectrochemistry, Ultrasonics, 2010, 50, 318-322.

[162]   Okitsu K., Iwatani M., Okano K.., Uddin Md.H., Nishimura R., Mechanism of sonochemical reduction of permanganate to manganese dioxide in aqueous alcohol solutions: Reactivities of reducing species formed by alcohol sonolysis, Ultrason. Sonochem., 2016, 31, 456-462.

[163]   Abulizi A., Yang G.H., Okitsu K., Zhu J.J., Synthesis of MnO_2 nanoparticles from sonochemical reduction of MnO_4 in water under different pH conditions, Ultrason. Sonochem., 2014, 21, 1629-1634.

[164]   Pol V.G., Grisaru H., Gedanken A., Coating noble metal nanocrystals (Ag, Au, Pd, and Pt) on polystyrene spheres via ultrasound irradiation, Langmuir: ACS J. Surf. Colloids, 2005, 21(8), 3635-40.

[165]   Pantidos N., Horsfall L.E., Biological Synthesis of Metallic Nanoparticles by Bacteria, Fungi and Plants, J. Nanomed. Nanotechnol., 2014, 5, 5.

[166]   Menon S., Rajeshkumar S., Venkat Kumar S., A review on biogenic synthesis of gold nanoparticles, characterization, and its applications, Resource-Efficient Technol., 2017, 3(4), 516-527.

[167]   Zha J., Dong C., Wang X., Zhang X., Xiao X., Yang X., Green synthesis and characterization of monodisperse gold nanoparticles using Ginkgo Biloba leaf extract, Optik, 2017, 144, 511-521.

[168]   Paulkumar K., Vanaja G.G.M., Rajeshkumar S., Malarkodi C., Pandian K., Annadurai G., Piper nigrum Leaf and Stem Assisted Green Synthesis of Silver Nanoparticles and Evaluation of Its Antibacterial Activity Against Agricultural Plant Pathogens, The Scientific World J., 2014, 829894.

[169]   Santhoshkumar J., Rajeshkumar S., Venkat-Kumar S., Phyto-assisted synthesis, characterization and applications of gold nanoparticles - A review, Biochemistry and Biophysics Reports, 2017, 11, 46-57.

[170]   Yan S., He W., Sun C., Zhang X., Zhao H., Li Z., Zhou W., Tian X., Sun X., Han X., The biomimetic synthesis of zinc phosphate nanoparticles, Dyes and Pigments, 2009, 80, 254-258.

[171]   Wang C., Xiao P., Zhao J., Zhao X., Liu Y., Wang Z., Biomimetic synthesis of hydrophobic calcium carbonate nanoparticles via a carbonation route, Powder Technol., 2006, 170, 31-35.

[172]   Li X., Xu H., Chen Z.S., Chen G., Biosynthesis of Nanoparticles by Microorganisms and Their Applications, J. Nanomaterials, 2011, Article ID 270974.

[173]   Show S., Tamang A., Chowdhury T., Mandal D., Chattopadhyay B., Bacterial (BKH1) assisted silica nanoparticles from silica rich-substrates: A facile and green approach for biotechnological applications, Colloids and Surfaces B: Biointerfaces, 2015, 126, 245-250.

[174]   Chokriwal A., Sharma M.M., Singh A., Biological Synthesis of Nanoparticles Using Bacteria and Their Applications, Am. J. PharmTech. Res., 2014, 4(6), ISSN: 2249-3387.

[175]   Fariq A., Tabeer K., Azra Y. Microbial synthesis of nanoparticles and their potential applications in biomedicine. J. Applied Biomedicine 2017; 15: 241-248.

[176]   Zielonka A., Klimek-Ochab M., Fungal synthesis of size-defined nanoparticles, Adv. Nat. Sci.: Nanosci. Nanotechnol., 2017, 8, 043001 (9pp).

[177]   Sharma D., Kanchi S., Bisetty K., Biogenic synthesis of nanoparticles: A review, Arabian J. Chemistry, 2019, 12(8), 3576-3600.

[178]   Stein A., Keller S.W., Mallouk T.E., Turning down the heat: design and mechanism in solid-state synthesis, Science, 1993, 259(5101), 1558-64.

[179]   Jansen M., A Concept for Synthesis Planning in Solid-State Chemistry, Angewandte Chemie Int. Edition, 2002, 41(20), 3746-3766.

[180]   Li Y., Cao Y., Jia D., A general strategy for synthesis of metal nanoparticles by a solid-state redox route under ambient conditions, J. Mater. Chem. A 2014, 11.

[181]   Supriya A., Patil S.A., Shinde D.V., Ahn D.Y., Patil D.V., Tehare K.K., Jadhav V.V., Lee J.K., Mane R.S., Shrestha N.K., Han S.H., A simple, room temperature, solid-state synthesis route for metal oxide nanostructures, J. Mater. Chem. A , 2014, 2, 13519-13526.

[182]   Wang Y., Zhang L., Li H., Wang Y., Jiao L., Yuan H., Chen L., Tang H., Yang X., Solid state synthesis of Fe2P nanoparticles as high-performance anode materials for nickel-based rechargeable batteries, J. Power Sources, 2014, 253, 360-365.

[183]   Wang L., Xi W., Mei T., Cai Y., Lu J., Zhao D., Huang H., Liu W., Zhou Q., Facile one-step solid-state reaction to synthesis of hafnium carbide nanoparticles at low temperature, J. Ceram. Soc. Jap.,

2017, 125(10), 789-791.

[184] Muthamizh S., Suresh R., Giribabu K., Manigandan R., Praveen-Kumar S., Solid state synthesis of copper tungstate nanoparticles and its electrochemical detection of 4-chlorophenol, AIP Conference Proceedings, 2014, 1591, 508.

[185] Tugova E.A., Gusarov V.V., Peculiarities of layered perovskite-related GdSrFeO$_4$ compound solid state synthesis, J. All. Comp., 2011, 509, 1523-1528.

[186] Wostek-Wojciechowska D., Jeszka J.K., Amiens C., Chaudret B., Lecante P., The solid-state synthesis of metal nanoparticles from organometallic precursors, J. Colloid Interf. Sci., 2005, 287(1), 107-113.

[187] Su X., Fu F., Yan Y., Zheng G., Liang T., Zhang Q., Cheng X., Yang D., Chi H., Tang X., Zhang Q., Uher C., Self-propagating high-temperature synthesis for compound thermoelectrics and new criterion for combustion processing, Nature Commun., 2014, 5, 4908.

[188] Subrahmanyam J., Vijayakumar M., Self-propagating high-temperature synthesis, J. Materials Science, 1992, 27, 6249-6273.

[189] Merzhanov A.G., The chemistry of self-propagating high-temperature synthesis, J. Mater. Chem., 2004, 14, 1779-1786.

[190] Huczko A., Kurcz M., Dabrowska A., Baranowski P., Bhattarai A., Gierlotka S., Self-propagating high-temperature synthesis (SHS) of crystalline nanomaterials, J. Crystal Growth, 2014, 401, 469-473.

[191] Mukasyan A.S., Rogachev A.S., Aruna S.T.R., Combustion synthesis in nanostructured reactive systems, Advanced Powder Technology, 2015, 26, 954-976.

[192] Xing T., Sunarso J., Yang W., Yin Y., Glushenkov A.M., Li L.H., Howlett P.C., Chen Y., One-step preparation of graphene nanosheets via ball milling of graphite and the application in lithium-ion batteries, Nanoscale, 2013, 5, 7970-7976.

[193] Tsuzuki T., McCormick P.G., Mechanochemical synthesis of nanoparticles, J. Mater. Sci., 2004, 39, 5143-5146.

[194] Wang H.S., Metal-organic frameworks for biosensing and bioimaging applications, Coord. Chem. Rev., 2017, 349, 139-155.

[195] Lu J., Ng K.M., Yang S., Efficient, One-Step Mechanochemical Process for the Synthesis of ZnO Nanoparticles, Ind. Eng. Chem. Res., 2008, 47, 1095-1101.

[196] Xu Ch., De S., Balu A.M., Ojeda M., Luque R., Mechanochemical synthesis of advanced nanomaterials for catalytic applications, Chem. Commun., 2015, 51, 6698-6713.

[197] Al-Kotb M.S., Selim H., Amer H.H., Khalil M.M., Kotkata M.F., Solid-state synthesis of ZnS nanoparticle via mechanical milling process, NSNTAIJ, 2014. 8(3).

[198] Urakaev F.K., Burkitbayev M.M., Tatykaev B., Uralbekov B., Mechanochemical Synthesis of Silver Chloride Nanoparticles by a Dilution Method in the System NH$_4$Cl - AgNO$_3$ - NH$_4$NO$_3$ system, Colloid J., 2015, 77(5), 641-65.

[199] Owens G.J., Singh R.K., Foroutan F., Alqaysi M., Han C.M., Mahapatra C., Kim H.W., Knowles J.C., Sol-gel based materials for biomedical applications, Progress in Materials Science, 2016, 77, 1-79.

[200] Qiao L., Swihart M.T., Solution-phase synthesis of transition metal oxide nanocrystals: Morphologies, formulae, and mechanisms, Adv. Colloid and Interf. Sci., 2017, 244, 199-266.

[201] Guo X., Zhang Q., Ding X., Shen Q., Wu C., Zhang L., Yang H., Synthesis and application of several sol-gel-derived materials via sol-gel process combining with other technologies: a review,

J. Sol-Gel. Sci. Technol., 2016, 79, 328-358.

[202] Schmidt H., Jonschker G., Goedicke S., Mennig M., The Sol-Gel Process as a Basic Technology for Nanoparticle-Dispersed Inorganic-Organic Composites, J. Sol-Gel Sci. Technol., 2000, 19, 39-51.

[203] Pierre A.C., Campet G., Han S.D., Duguet E., Portier J., TiO$_2$-Polymer Nano-Composites by Sol-Gel. J. Sol-Gel Sci. Technol., 1994, 2, 121-125.

[204] Bae C., Yoo H., Kim S., Lee K., Kim J., Sung M.M., Shin H., Template-Directed Synthesis of Oxide Nanotubes: Fabrication, Characterization, and Applications, Chem. Mater., 2008, 20, 756-767.

[205] Mann S., Burkett S.L., Davis S.A., Fowler C.E., Mendelson N.H., Sims S.D., Walsh D., Whilton N.T., Sol-Gel Synthesis of Organized Matter, Chem. Mater., 1997, 9, 2300-2310.

[206] Sakka S., The Current State of Sol-Gel Technology, J. Sol-Gel Sci. Technol., 1994, 3, 69-81.

[207] Giordano C., Antonietti M., Synthesis of crystalline metal nitride and metal carbide nanostructures by sol-gel chemistry, Nano Today, 2011, 6, 366-380.

[208] Cordoncillo E., Carda J.B., Tena M.A., Monros G., Escribano P., Synthesis of Quantum-Size Cadmium-Zinc Sulfide Particle-Doped Glasses by the Sol-Gel Method, J. Sol-Gel Sci. Technol., 1997, 8, 1043-1047.

[209] Sumida K., Liang K., Reboul J., Ibarra I.A., Furukawa S., Falcaro P., Sol-Gel Processing of Metal-Organic Frameworks, Chem. Mater., 2017, 29, 2626-2645.

[210] Pechini M.P., Method of preparing lead and alkaline earth titanates and niobates and coating method using the same to form a capacitor, Patent US 3330697 A, 1967.

[211] Grzyb T., Lis S., Structural and Spectroscopic Properties of LaOF:Eu^{3+} Nanocrystals Prepared by the Sol Gel Pechini Method, Inorg. Chem., 2011, 50, 8112-8120.

[212] Grzyb T., Szczeszak A., Rozowska J., Legendziewicz J., Li S., Tunable Luminescence of Sr$_2$CeO$_4$:M^{2+}(M = Ca, Mg, Ba, Zn) and Sr$_2$CeO$_4$:Ln^{3+}(Ln = Eu, Dy, Tm) Nanophosphors, J. Phys. Chem. C, 2012, 116, 3219-3226.

[213] Bieza M., Guzik M., Tomaszewicz E., Guyot Y., Lebbou K., Boulon G., Toward Optical Ceramics Based on Yb^{3+} Rare Earth Ion-Doped Mixed Molybdato-Tungstates: Part II - Spectroscopic Characterization, J. Phys. Chem. C, 2017, 121, 13303-13313.

[214] Cheetham A.K., Mellot C.F., In Situ Studies of the Sol-Gel Synthesis of Materials, Chem. Mater., 1997, 9, 2269-2279.

[215] Demazeau G., Solvothermal and hydrothermal processes: the main physico-chemical factors involved and new trends, Res. Chem. Intermed., 2011, 37, 107-123.

[216] Yoshimura M., Byrappa K., Hydrothermal processing of materials: past, present and future, J. Mater. Sci., 2008, 43, 2085-2103.

[217] Gao S., Lu J., Zhao Y., Chen N., Xie Y., The Growth Process, Stability of GaP Nanocrystals and Formation of Ga$_3$P Nanocrystals under Solvothermal Conditions in Benzene, Eur. J. Inorg. Chem., 2003, 9, 1822-1827.

[218] Lai J., Niu W., Luque R., Xu G., Solvothermal synthesis of metal nanocrystals and their applications, Nano Today, 2015, 10, 240-267.

[219] Plumley A.L., A Simplified Bomb for Hydrothermal Synthesis, J. Chem. Educ., 1960, 37(4), 201.

[220] Byrappa K., Adschiri T., Hydrothermal technology for nanotechnology, Progress in Crystal Growth and Characterization of Materials, 2007, 53, 117-166.

[221] Byrappa K., Keerthiraj N., Byrappa S.M., Handbook of Crystal Growth, Elsevier B.V., 2015, 535-575.

[222] Somiya S., Rustum R., Hydrothermal synthesis of fine oxide powders, Bull. Mater. Sci., 2000, 23(6), 453-460.

[223] Shevchenko A.V., Ruban A.K., Dudnik E.V., Melnikova V.A., Hydrothermal synthesis of ultrafine zirconia powders, Powder Metallurgy and Metal Ceramics, 1997, 36, 7-8.

[224] Feng S., Xu R., New Materials in Hydrothermal Synthesis, Acc. Chem. Res., 2001, 34, 239-247.

[225] Byrappa K., Yoshimura M., Handbook of Hydrothermal Technology, Elsevier, 2001.

[226] Lai J., Niu W., Luque R., Xu G., Solvothermal synthesis of metal nanocrystals and their applications, Nano Today, 2015, 10, 240-267.

[227] Nadimpalli N.K.V., Bandyopadhyaya R., Runkana V., Thermodynamic analysis of hydrothermal synthesis of nanoparticles, Fluid Phase Equilibria, 2018, 456, 33-45.

[228] Darr J.A., Zhang J., Makwana N.M., Weng X., Continuous Hydrothermal Synthesis of Inorganic Nanoparticles: Applications and Future Directions, Chem. Rev., 2017, 117, 11125-11238.

[229] Adschiri T., Hakuta Y., Sue K., Arai K., Hydrothermal synthesis of metal oxide nanoparticles at supercritical conditions, J. Nanopart. Res., 2001, 3, 227-235.

[230] Brill T.B., Geothermal Vents and Chemical Processing: The Infrared Spectroscopy of Hydrothermal Reactions, J. Phys. Chem. A, 2000, 104, 4343-4351.

[231] Tekin K., Karagoz S., Bektas S., A review of hydrothermal biomass processing, Renew. Sustain. Energy Rev., 2014, 40, 673-687.

[232] Rao K.J., Vaidhyanathan B., Ganguli M., Ramakrishnan P.A., Synthesis of Inorganic Solids Using Microwaves, Chem. Mater., 1999, 11, 882-895.

[233] Kim J., Mun S.C., Ko H.I., Kim K.B., Khondoker M.A.H., Zhai L., Review of Microwave Assisted Manufacturing Technologies, Int. J. Prec. Eng. Manuf., 2012, 13(12), 2263-2272.

[234] Vaidhyanathan B., Balaji K., Rao K.J., Microwave-Assisted Solid-State Synthesis of Oxide Ion Conducting Stabilized Bismuth Vanadate Phases, Chem. Mater., 1998, 10, 3400-3404.

[235] Shen H., Xue T., Wang Y., Cao G., Lu Y., Fang G., Photocatalytic property of perovskite $LaFeO_3$ synthesized by sol-gel process and vacuum microwave calcination, Mater. Res. Bulletin, 2016, 84, 15-24.

[236] Guo S., Dai Q., Wang Z., Yao H., Rapid microwave irradiation synthesis of carbon nanotubes on graphite surface and its application on asphalt reinforcement, Composites Part B, 2017, 124, 134-143.

[237] Gajengi A.L., Sasaki T., Bhanage B.M., Mechanistic aspects of formation of MgO nanoparticles under microwave irradiation and its catalytic application, Adv. Powder Technol., 2017, 28, 1185-1192.

[238] Singh S., Sabri Y.M., Jampaiah D., Selvakannan P.R., Nafady A., Kandjani A.E., Bhargava S.K., Easy, one-step synthesis of CdTe quantum dots via microwave irradiation for fingerprinting application, Mater. Res. Bulletin, 2017, 90, 260-265.

[239] Quan Z., Yang P., Li C., Yang J., Yang D., Jin Y., Lian H., Li H., Lin J., Shape and Phase-Controlled Synthesis of $KMgF_3$ Colloidal Nanocrystals via Microwave Irradiation, J. Phys. Chem. C, 2009, 113, 4018-4025.

[240] Roy E., Patra S., Saha S., Madhuri R., Sharma P.K., Shape-specific silver nanoparticles prepared by microwave-assisted green synthesis using pomegranate juice for bacterial inactivation and removal, RSC Adv., 2015, 5, 95433.

[241] Fatimah I., Green synthesis of silver nanoparticles using extract of Parkia speciosa Hassk pods assisted by microwave irradiation, J. Adv. Res., 2016, 7, 961-969.

[242] Hasanpoor M., Nabavi H.F., Aliofkhazraei M., Microwave-Assisted Synthesis of Alumina Nanoparticles Using Some Plants Extracts, J. Nanostruct., 2017, 7(1), 40-46.

[243] Vollath D., Plasma synthesis of nanopowders, J. Nanopart. Res., 2008, 10, 39-57.

[244] Wangensteen T., Dhakal T., Merlak M., Mukherjee P., Phan M.H., Chandra S., Srikanth H., Witanachchi S., Growth of uniform ZnO nanoparticles by a microwave plasma process, J. All. Comp., 2011, 509, 6859-6863.

[245] Zhen Q., Kale G.M., He W., Liu J., Microwave Plasma Sintered Nanocrystalline Bi_2O_3-HfO_2-Y_2O_3 Composite Solid Electrolyte, Chem. Mater., 2007, 19, 203-210.

[246] Bogdanowicz R., Sawczak M., Niedzialkowski P., Zieba P., Finke B., Ryl J., Karczewski J., Ossowski T., Novel Functionalization of Boron-Doped Diamond by Microwave Pulsed-Plasma Polymerized Allylamine Film, J. Phys. Chem. C, 2014, 118, 8014-8025.

[247] Irzh A., Genish I., Klein L., Solovyov L.A., Gedanken A., Synthesis of ZnO and Zn Nanoparticles in Microwave Plasma and Their Deposition on Glass Slides, Langmuir, 2010, 26(8), 5976-5984.

[248] Mingos D.M.P., Baghurst D.R., Applications of microwave dielectric heating effects to synthetic problems in chemistry, Chemical Society Reviews, 1991, 20, 1-47.

[249] Mingos D.M.P., The applications of microwaves in chemical syntheses, Res. Chem. Intermed., 1994, 20, 85-91.

[250] Qun X., Jiajia J., Shanyu Z., Pinghua Z., Haixun X., Microwave-assisted Hydrothermal Synthesis of Carbon Materials with Tunable Microstructure, J. Wuhan University of Technology-Mater. Sci. Ed., 2017, 32(5), 1032-1037.

[251] Deekamwong K., Kaiyasuan C., Jitcharoen J., Wittayakun J., Influence of gel composition and microwave-assisted hydrothermal time in MCM-41 synthesis, Mater. Chem. and Physics, 2017, 201, 384-390.

[252] Kee L.H., Chyi lj.Y., Talib Z.A., Mamat M.S., Ngee J.L.H., Ashari F., AL-Jumaili B.E., Huang L.Z., Hasbullah N.N., Optical characterization of zinc selenide/grapheneoxide composite synthesized via microwave assisted hydrothermal method, Optik, 2017, 144, 49-53.

[253] Li Z., Chen Y., Li J.F., Chen H., Wang L., Zheng S., Lu G., Systhesizing SnTe nanocrystals leading to thermoelectric performance enhancement via an ultra-fast microwave hydrothermal method, Nano Energy, 2016, 28, 78-86.

[254] Smolen D., Chudoba T., Gierlotka S., Kedzierska A., Lojkowski W., Sobczak K., Swieszkowski W., Kurzydlowski K.J., Hydroxyapatite Nanopowder Synthesis with a Programmed Resorption Rate, J. Nanomaterials, 2012, Article ID 841971, 9pp.

[255] Witkowski B.S., Wachnicki L., Gieraltowska S., Dluzewski P., Szczepanska A., Kaszewski J., Godlewski M., Ultra-fast growth of the monocrystalline zinc oxide nanorods from the aqueous solution, Int. J. Nanotechnol., 2014, 11, 758-772.

[256] Strachowski T., Grzanka E., Palosz B.F., Presz A., Slusarski L., Lojkowski W., Microwave Driven Hydrothermal Synthesis of Zinc Oxide Nanopowders, Solid State Phenomena, 2003, 94, 189-192.

[257] Kaszewski J., Yatsunenko S., Pelech I., Mijowska E., Narkiewicz U., Godlewski M., High pressure synthesis versus calcination - different approaches to crystallization of zirconium dioxide,

Polish J. Chemical Technology, 2014, 16(2), 99-105.

[258] Kaszewski J., Lojkowski W., Narkiewicz U., Preparation of ZrO_2:Tb via microwave hydrothermal metod, Optica Applicata, 2009, 39(4).

[259] Wolska-Kornio E., Kaszewski J., Witkowski B.S., Wachnicki L., Godlewski M., The effect of annealing on properties of europium doped ZnO nanopowders obtained by a microwave hydrothermal method, Optical Mater., 2016, 59, 103-106.

[260] Fidelus J.D., Yatsunenko S., Godlewski M., Paszkowicz W., Werner-Malento E., Lojkowski W., Relation between structural properties of Pr^{3+}-doped yttria-stabilized zirconia nanopowders and their luminescence efficiency, Scripta Materialia, 2009, 61, 415-418.

[261] Bondioli F., Ferrari A.M., Braccini S., Leonelli C., Pellacani G.C., Opalinska A., Chudoba T., Grzanka E., Palosz B.F., Lojkowski W., Microwave - Hydrothermal Synthesis of Nanocrystalline Pr - Doped Zirconia Powders at Pressures up to 8 MPa, Solid State Phenomena, 2003, 94, 193-196.

[262] Rosowska J., Kaszewski J., Witkowski B.S., Wachnicki L., Godlewski M., The Effect of Synthesis Pressure on Properties of Eu-Doped ZnO Nanopowders Prepared by Microwave Hydrothermal Method, Acta Phys. Pol. A, 2016, 130(5), 1205-1208.

[263] Yatsunenko S., Kaszewski J., Grzyb J., Pelech I., Godlewski M.M., Mijowska E., Narkiewicz U., Godlewski M., Impact of yttria stabilization on Tb^{3+} intra-shell luminescence efficiency in zirconium dioxide nanopowders, J. Phys.: Condens. Matter, 2013, 25, 194106.

[264] Kaszewski J., Witkowski B.S., Wachnicki L., Przybylinska H., Kozankiewicz B., Mijowska E., Godlewski M., Luminescence enhancement in nanocrystalline Eu_2O_3 nanorods - Microwave hydrothermal crystallization and thermal degradation of cubic phase, Optical Mater., 2016, 59, 76-82.

[265] Godlewski M., Yatsunenko S., Nadolska A., Opalinska A., Lojkowski W., Drozdowicz-Tomsia K., Goldys E.M., Nanoparticles doped with TM and RE ions for applications in optoelectronics, Optical Mater., 2009, 31, 490-495.

[266] Godlewski M., Wolska E., Yatsunenko S., Opalinska A., Fidelus J., Lojkowski W., Zalewska M., Klonkowski A., Kuritsyn D., Doped nanoparticles for optoelectronics applications, Low Temp. Phys., 2009, 35, 48.

[267] Tomaszewska-Grzeda A., Opalinska A., Grzanka E., Lojkowski W., Gedanken A., Godlewski M., Yatsunenko S., Osinniy V., Story T., Magnetic properties of ZnMnO nanopowders solvothermally grown at low temperature from zinc and manganese acetate, Appl. Phys. Lett., 2006, 89, 242102.

[268] Sibera D., Jedrzejewski R., Mizeracki J., Presz A., Narkiewicz U., Lojkowski W., Synthesis and Characterization of ZnO Doped with Fe_2O_3 - Hydrothermal Synthesis and Calcination Process, Acta Phys. Pol. A, 2009, 116, 133.

[269] Kaszewski J., Witkowski B.S., Wachnicki L., Przybylinska H., Kozankiewicz B., Mijowska E., Godlewski M., Reduction of Tb^{4+} ions in luminescent Y_2O_3:Tb nanorods prepared by microwave hydrothermal method, J. Rare Earths, 2016, 34(8), 774-781.

[270] Wolska E., Kaszewski J., Kielbik P., Grzyb J., Godlewski M.M., Godlewski M., Rare earth activated ZnO nanoparticles as biomarkers, Optical Mater., 2014, 36, 1655-1659.

[271] Kaszewski J., Godlewski M.M., Witkowski B.S., Slonska A., Wolska-Kornio E., Wachnicki L., Przybylinska H., Kozankiewicz B., Szal A., Domino M.A., Mijowska E., Godlewski M., Y_2O_3:Eu nanocrystals as biomarkers prepared by a microwave hydrother-

mal method, Optical Mater., 2016, 59, 157-164.

[272] Kaszewski J., Borgstrom E., Witkowski B.S., Wachnicki L., Kielbik P., Slonska A., Domino M.A., Narkiewicz U., Gajewski Z., Hochepied J.F., Godlewski M.M., Godlewski M., Terbium content affects the luminescence properties of ZrO_2:Tb nanoparticles for mammary cancer imaging in mice, Optical Mater., 2017, 74, 16-26.

[273] Lipinski W., Kaszewski J., Gajewski Z., Godlewski M., Godlewski M.M., Wide band-gap oxides nanoparticles as potential drug carriers, Med. Weter., 2017, 73(10), 657-660.

[274] Lojkowski W., Gedanken A., Grzanka E., Opalinska A., Strachowski T., Pielaszek R., Tomaszewska-Grzeda A., Yatsunenko S., Godlewski M., Matysiak H., Kurzydlowski K.J., Solvothermal synthesis of nanocrystalline zinc oxide doped with Mn^{2+}, Ni^{2+}, Co^{2+} and Cr^{3+} ions, J. Nanopart. Res., 2009, 11, 1991-2002.

[275] Wolska E., Witkowski B.S., Godlewski M., ZnO Nanopowders by a Microwave Hydrothermal Method - Influence of the Precursor Type on Grain Sizes, Acta Phys. Pol. A. 2011, 5(119), 683-685.

[276] Wolska E., Sibera D., Witkowski B.S., Yatsunenko S.A., Pelech I., Narkiewicz U., Godlewski M., Photoluminescence and Chromaticity Properties of ZnO Nanopowders Made by a Microwave Hydrothermal Method, Acta Phys. Pol. A, 2011, 5(120), 908-910.

[277] Aimable A., Strachowski T., Wolska E., Lojkowski W., Bowen P., Comparison of two innovative precipitation systems for ZnO and Al-doped ZnO nanoparticle synthesis, Proces. Appl. Ceram., 2010, 4(3), 107-114.

[278] Zawadzki M., Synthesis of nanosized and microporous zinc aluminate spinel by microwave assisted hydrothermal method (microwave-hydrothermal synthesis of $ZnAl_2O_4$), Solid State Sciences, 2006, 8, 14-18.

[279] Sibera D., Strachowski T., Lojkowski W., Narkiewicz U., Chudoba T., Jedrzejewski R., Majcher A., Presz A., Nano-$ZnAl_2O_4$ - Hydrothermal MW Assisted Synthesis in a Stop-Flow Reactor and Characterization, Maintenance Problems, 2010, 4, 91-102.

[280] Fidelus D., Jojkowski W., Millers D., Grigorjeva L., Smits K., Piticescu R.R., Zirconia Based Nanomaterials for Oxygen Sensors - Generation, Characterisation and Optical Properties, Solid State Phenomena, 2007, 128, 141-150.

[281] Smits K., Grigorjeva L., Millers D, Sarakovskis A., Opalinska A., Fidelus J.D., Lojkowski W., Europium doped zirconia luminescence, Optical Mater., 2010, 32, 827-831.

[282] Yatsunenko S., Kaszewski J., Grzyb J., Pelech I., Godlewski M.M., Mijowska E., Narkiewicz U., Godlewski M., Impact of yttria stabilization on Tb^{3+} intra-shell luminescence efficiency in zirconium dioxide nanopowders, J. Phys.: Condens. Matter, 2013, 25, 194106.

[283] Massoud T.F., Gambhir S.S., Molecular imaging in living subjects: seeing fundamental biological processes in a new light, Genes Dev., 2003, 17, 545-580.

[284] Runge V.M., Stewart R.G., Clanton J.A., Jones M.M., Lukehart C.M., Partain C.L., James A.E.Jr., Work In progress: potential oral and intravenous paramagnetic NMR contrast agents, Radiology, 1983, 147(3), 789-91.

[285] Zhou Z., Lu Z.R., Gadolinium-Based Contrast Agents for MR Cancer Imaging, Wiley Interdiscip. Rev. Nanomed. Nanobiotechnol., 2013, 5(1), 1-18.

[286] Hadizadeh D.R., Von F.M., Kukuk G.M., Schoneseiffen K., Gieseke J., Schild H.H., Willinek W.A., Contrast material for abdominal dynamic contrast-enhanced 3D MR angiography with parallel imaging: intraindividual equimolar comparison of a

macrocyclic 1.0 M gadolinium chelate and a linear ionic 0.5 M gadolinium chelate, AJR Am. J. Roentgenol., 2010, 194, 821-829.

[287] Essig M., Shiroishi M.S., Nguyen T.B., Saake M., Provenzale J.M., Enterline D., Anzalone N., Dorfler A., Rovira A., Wintermark M., Law M., MRI: the five most frequently asked technical questions, AJR Am. J. Roentgenol., 2013, 200, 20024-20034.

[288] Lin S.P., Brown J.J., MR contrast agents: physical and pharma-cologic basics, J. Magn. Reson. Imaging., 2007, 25(5), 884-99.

[289] ACR - American College of Radiology. Manual on Contrast Media: Nephrogenic Systemic Fibrosis, 2015, 83-91, 2015. Available via: http://www.acr.org/qualitysafety/resources/~/media/37D84428BF1D4E1B9A3A2468DA4EWAiandson Accessed 18 Jan 2016

[290] Dosa E., Guillaume D.J., Haluska M., Lacy C., Hamilton B., Njus J.M., Rooney W.D., Kraemer D.F., Muldoon L., Neuwelt E.A., Mag-netic resonance imaging of intracranial tumors: Intra-patient comparison of gadoteridol and ferumoxytol, Neuro-oncol., 2011, 13(2), 251-260.

[291] Davenport M.S., Dillman J.R., Cohan R.H., Hussain H.K., Kha-latbari S., McHugh J.B., Ellis J.H., Effect of abrupt substitution of gadobenate dimeglumine for gadopentetate dimeglumine on rate of allergic-like reactions, Radiology, 2013, 266, 773-82.

[292] Tweedle M.F., Runge V.M., Gadoteridol., Drugs of the Future, 1992, 17, 187.

[293] Cacheris W.P., Quary S.C., Rocklage S.M., The relationship be-tween thermodynamics and the toxicity of gadolinium complexes, Magn. Reson. Imaging, 1990, 8, 467-481.

[294] Kirchin M.A., Runge V.M., Contrast agents for magnetic reso-nance imaging: safety update, Topics in Magnetic Resonance Imaging, 2003, 14(5), 426-435.

[295] Tweedle M.F., Wedeking P., Kumar K., Biodistribution of radi-olabeled, formulated gadopentetate, gadoteridol, gadoterate, and gadodiamide in mice and rats, Investig. Radiol., 1995, 30(6), 372-380.

[296] Morcos S.K., Extracellular gadolinium contrast agents: differ-ences in stability, European J. Radiology, 2008, 66(2), 175-179.

[297] Corot C., Idee J.M., Hentsch A.M., Santus R., Mallet C., Goulas V., Bonnemain B., Meyer D., Structure-activity relationship of macrocyclic and linear gadolinium chelates: investigation of transmetallation effect on the zinc-dependent metallopeptidase angiotensin-converting enzyme, J. Magnetic Resonance Imaging, 1998, 8(3), 695-702.

[298] Grobner T., Gadolinium - a specific trigger for the development of nephrogenic fibrosing dermopathy and nephrogenic systemic fibrosis, Nephrol. Dial. Transplant., 2006, 21(4), 1104-1108.

[299] Pietsch H., Lengsfeld P., Jost G., Frenzel T., Hutter J., Sieber M.A., Long-term retention of gadolinium in the skin of rodents follow-ing the administration of gadolinium-based contrast agents, Eur Radiol., 2009, 19(6), 1417-1424.

[300] Pietsch H., Lengsfeld P., Steger-Hartmann T., Lowe A., Frenzel T., Hutter J., Sieber M., Impact of renal impairment on long-term retention of gadolinium in the rodent skin following the admin-istration of gadolinium-based contrast agents, Invest. Radiol., 2009, 44(4), 226-233.

[301] Pietsch H., Pering C. Lengsfeld P., Walter J., Steger-Hartmann T., Golfier S., Frenzel T., Hutter J., Weinmann H.J., Sieber M.A., Evaluating the role of zinc in the occurrence of fibrosis of the skin: a preclinical study, J. Magn. Reson. Imaging., 2009, 30(2), 374-383.

[302] Pietsch H., Raschke M., Ellinger-Ziegelbauer H., Jost G., Wal-ter J., Frenzel T., Lenhard D., Hutter J., Sieber M.A., The role of

residual gadolinium in the induction of nephrogenic systemic fibrosis-like skin lesions in rats, Invest. Radiol., 2011, 46(1), 48-56.

[303] Kanda T., Fukusato T., Matsuda M., Toyoda K., Oba H., Kotoku J., Haruyama T., Kitajima K., Furui S., Gadolinium-based contrast agent accumulates in the brain even in subjects without severe renal dysfunction: evaluation of autopsy brain specimens with inductively coupled plasma mass spectroscopy, Radiology, 2015, 276(1), 228-232.

[304] McDonald R.J., McDonald J.S., Kallmes D.F., Jentoft M.E., Murray D.L., Williamson E.E., Eckel L.J., Intracranial gadolin-ium deposition after contrast-enhanced MR imaging, Radiology, 2015, 275(3), 772-782.

[305] Kanal E., Tweedle M.F., Residual or retained gadolinium: prac-tical implications for radiologists and our patients, Radiology, 2015, 275(3), 630-634.

[306] EMA- European Medicines Agency, EMA/486286/2012, London, UK: European Medicines Agency, 2012.

[307] Terreno E., Castelli D.Di., Viale A., Aime S., Challenges for molec-ular magnetic resonance imaging, Chem. Rev., 2010, 110, 3019-3042.

[308] Kim T., Momin E., Choi J., Yuan K., Zaidi H., Kim J., Park M., Lee N., McMahon M.T., Quinones-Hinojosa A., Bulte J.W.M., Hyeon T., Gilad A.A., Mesoporous silica-coated hollow manganese oxide nanoparticles as positive T1 contrast agents for labeling and MRI tracking of adipose-derived mesenchymal stem cells, J. Am. Chem. Soc., 2011, 133, 2955-2961.

[309] Bulte J.W.M., Kraitchman D.L., Iron oxide MR contrast agents for molecular and cellular imaging, NMR Biomed., 2004, 17(7), 484-99.

[310] Zhang F., Huang X., Qian C., Zhu L., Hida N., Niu G., Chen X., Syn-ergistic enhancement of iron oxide nanoparticle and gadolinium for dual-contrast MRI, Biochem. Biophys. Res. Commun., 2012, 425, 886-891.

[311] Singh N., Jenkins G.J.S., Asadi R., Doaka S.H., Potential toxicity of superparamagnetic iron oxide nanoparticles (SPION), Nano Reviews, 2010, 1, 5358.

[312] Wei Y., Zhao M., Yang F., Mao Y., Xie H., Zhou Q., Iron overload by Superparamagnetic Iron Oxide Nanoparticles is a High Risk Factor in Cirrhosis by a Systems Toxicology Assessment, Sci. Rep., 2016, 6, 29110.

[313] Lam T., Pouliot P., Avti P.K., Lesage F., Kakkar A.K., Superparam-agnetic iron oxide based nanoprobes for imaging and theranos-tics, Adv. Colloid. Interface. Sci., 2013, 199-200, 95-113.

[314] Li Z., Yi P.W., Sun Q., Lei H., Zhao H.L., Zhu Z.H., Smith S.C., Lan M.B., Lu G.Q.M., Ultrasmall Water-Soluble and Biocompatible Magnetic Iron Oxide Nanoparticles, Adv. Funct. Mater., 2012, 22(11), 2387-2393.

[315] Baptista P.V., Quaresma P., Franco R., Nanoparticles in molecular diagnostics, Prog. Mol. Biol. Transl. Sci., 2011, 104, 427-488.

[316] Babayevska N., Florczak P., Wozniak-Budych M., Jarek M., Nowaczyk G., Zalewski T., Jurga S., Functionalized multimodal ZnO@Gd$_2$O$_3$ nanosystems to use as perspective contrast agent for MRI, Appl. Surf. Sci., 2017, 404, 129-137.

[317] Zeng X., Yuan J., Wang Z., Zhang L., Nanosheet-Based Micro-spheres of Eu^{3+}-doped ZnO with Efficient Energy Transfer from ZnO to Eu^{3+} at Room Temperature, Adv. Mater., 2007, 19, 4510-4514.

[318] Zeng X., Yuan J., Zhang L., Synthesis and Photoluminescent Properties of Rare Earth Doped ZnO Hierarchical Microspheres, J.

Phys. Chem. C, 2008, 112, 3503-3508.

[319] Geburt S., Lorke M., da Rosa A.L., Frauenheim T., Roder R., Voss T., Kaiser U., Heimbrodt W., Ronning C., Intense Intrashell Luminescence of Eu-Doped Single ZnO Nanowires at Room Temperature by Implantation Created Eu-Oi Complexes, Nano Lett., 2014, 14, 4523-4528.

[320] Gerigk M., Ehrenreich P., Wagner M.R., Wimmer I., Reparaz J.S., Sotomayor-Torres C.M., Schmidt-Mende L., Polarz S., Nanoparticle shape anisotropy and photoluminescence properties: Europium containing ZnO as a Model Case, Nanoscale, 2015, 7, 16969-16982.

[321] Ishizumi A., Kanemitsu Y., Structural and luminescence properties of Eu-doped ZnO nanorods fabricated by a microemulsion method, Appl. Phys. Lett., 2005, 86, 253106.

[322] Hayashi Y., Narahara H., Uchida T., Noguchi T., Ibuki S., Photoluminescence of Eu-Doped ZnO Phosphors, Jpn. J. Appl. Phys., 1995, 34(1), 1878.

[323] Yang L., Dong J., She Y., Jiang Z., Zhang L., Yu H., Self-purification construction of interstitial O in the neighbor of Eu^{3+} ions to act as energy transfer bridge, Appl. Phys. Lett., 2014, 104, 033109.